COPY NO. 12

TECHNICAL REPORT 3893

THE EFFECTS OF REACTOR IRRADIATION ON THE CHEMICAL CHARACTERISTICS OF SOLID EXPLOSIVES

CHARLES RIBAUDO
JAMES MALLAY
HAROLD J. MATSUGUMA

JANUARY 1970

PICATINNY ARSENAL
DOVER, NEW JERSEY

Technical Report 3893

THE EFFECTS OF REACTOR IRRADIATION ON THE CHEMICAL CHARACTERISTICS OF SOLID EXPLOSIVES

by

Charles Ribaudo
James Mallay
Harold J. Matsuguma

January 1970

Explosives Laboratory
Feltman Research Laboratories
Picatinny Arsenal
Dover, New Jersey

The citation in this report of the trade names of commercially available products does not constitute official indorsement or approval of the use of such products.

TABLE OF CONTENTS

	Page
Abstract	1
Introduction	2
Experimental Procedures	2
Explosives and Propellants	2
Irradiation Procedure	2
Analysis of Irradiated Material	2
Results	4
Infrared Spectrophotometric Analysis	4
Differential Thermal Analysis (DTA)	5
X-ray Diffraction Analysis	5
Melting Point Determination	5
Viscosity Measurements	5
Ultraviolet Spectrophotometric Examination	5
Discussion of Results	6
Effects of Irradiation	6
Chemical Stability	9
Acknowledgements	10
References	10
Distribution List	67
Tables	
1 Material irradiated in a high flux test reactor	12
2 Infrared spectral data for irradiated TNT	13
3 Infrared spectral data for irradiated HMX/EXON	14
4 Infrared spectral data for irradiated DATB	15
5 Infrared spectral data for irradiated PETN	16

Page

Tables

6 Differential thermal analysis data for irradiated TNT, HMX/EXON, DATB and PETN 17

7 X-ray diffraction data for irradiated explosives interplanar spacings in Å 18

8 Melting point data for irradiated TNT, DATB and PETN 19

9 Propellant viscosities 20

10 Summary of analytical data obtained for irradiated explosives 21

Figures

1 Infrared spectra for irradiated and standard TNT 22

2 Infrared spectra for irradiated and standard HMX/EXON (9505) 23

3 Infrared spectra for irradiated and standard DATB 24

4 Infrared spectra for irradiated and standard PETN 26

5 DTA curves for irradiated and standard TNT 28

6 DTA curves for irradiated and standard HMX/EXON (9505) 32

7 DTA curves for irradiated and standard PETN 41

8 DTA curves for irradiated and standard DATP 50

9 X-ray diffractograms for irradiated and standard TNT 57

Page

Figures

10	X-ray diffractograms for irradiated and standard HMX/EXON (9505)	58
11	X-ray diffractograms for irradiated and standard DATB	59
12	X-ray diffractograms for irradiated and standard PETN	61
13	Ultraviolet spectra for irradiated and standard propellants	63

BLANK PAGE

ABSTRACT

A study was made of TNT, HMX/EXON (9505), DATB, and PETN which had been irradiated in a nuclear reactor to determine chemical changes induced by the irradiation. Chemical changes (stability) were determined by infrared spectrophotometric, x-ray diffraction, and differential thermal analysis of the post-irradiated explosives. In addition, a similar study of nitrocellulose-base propellants was carried out. From the data obtained, the order of decreasing chemical stability under irradiation was DATB, HMX/EXON, TNT, PETN, and the nitrocellulose-base propellants; DATB was found to be the most stable.

INTRODUCTION

Several years ago, a program was initiated to study the effects of nuclear radiation on explosives and propellants. The program was carried out jointly by the Aerojet General Corporation and Picatinny Arsenal under the sponsorship of the National Aeronautics and Space Administration--SNPO--Cleveland Extension. In the initial phase of the program, a number of explosives and propellants were irradiated in a high flux test reactor at the General Electric Company site in Pleasanton, California. Physical testing was normally done within 24 hours of irradiation at the reactor site. Portions of the irradiated samples remaining after testing at the reactor site were sent to Picatinny for further study. Such study involved the determination of the effects of the irradiation on the chemical characteristics of the materials irradiated and the correlation of these effects with the chemical stability of the materials. The results of this study were initially submitted to Aerojet General Corporation for a combined report to NASA-SNPO-C (Ref 1) and are now reproduced in this report with some minor revisions.

EXPERIMENTAL PROCEDURES

Explosives and Propellants

The history of the materials used for irradiation is described in References 1 and 2. Samples of the irradiated materials which were shipped from the reactor site to Picatinny are listed in Table 1 together with their radiation histories (summarized). The nonirradiated explosives and propellants (standards) used in this study were obtained at Picatinny and were considered acceptable in accordance with the relevant military specifications.

Irradiation Procedure

The procedures and type of reactor used are described in detail in References 1 and 2.

Analysis of Irradiated Material

Melting Point Determination

The apparatus used for this determination was the Thomas-Hoover Melting Point Apparatus ("Uni-Melt") which uses G.E. SF 96 (50) silicone fluid for the temperature

bath and borosilicate capillary tubes for the sample holders.

Infrared Spectrophotometric Analysis

The instrument used in the infrared examination of the irradiated material was a double-beam recording infrared spectrophotometer, Perkin Elmer Corporation Model 21. The potassium bromide (KBr) pellet technique was used for the preparation of the irradiated sample for subsequent infrared examination. The spectra of the irradiated samples were compared to those of the standard material.

X-Ray Diffraction Analysis

The equipment used in the x-ray diffraction examination of the irradiated material was a Geiger counter, an X-Ray diffractometer (North American Phillips Inc.), a Brown potentiometer automatic recorder, and a copper x-ray tube with a nickel filter.

Differential Thermal Analysis (DTA)

The apparatus and procedure used to obtain the DTA curves of the irradiated and nonirradiated explosives are similar to those described in Reference 3. The DTA curve of the irradiated sample was compared to that of a standard sample of the same material.

Viscosity Measurements

The apparatus and procedure used for viscosity measurements are described in Reference 4.

Ultraviolet Spectrophotometric Examination

The instrument used in the ultraviolet spectrophotometric examination was a Cary recording quartz spectrophotometer, Applied Physics Corporation Model 11. An ethyl alcohol solution of the irradiated propellant sample, 0.25% nitrocellulose content, was prepared for examination.

A nonirradiated sample of the same propellant was similarly treated and the resulting curve compared to that obtained for the irradiated sample.

RESULTS

Infrared Spectrophotometric Analysis

A compilation of infrared spectral data for samples of TNT, DATB, HMX/EXON, and PETN, irradiated at various dose levels and exposure times, is given in Tables 2 through 5. Spectral data for nonirradiated standard explosive samples is included in each table.

Figures 1 through 4 show the infrared spectra for irradiated samples A11, A13, A21, B13, B21, C13, C22, C23, D12, D14, D21, and D25 together with spectra for the respective standards. Each of the irradiated sample spectra is designated as the representative spectrum (except A21) for the group of samples irradiated at the same dose level and exposure time as indicated below.

		Dose Level		
Explosive	Sample No.	γ-ray $\times 10^{-8}$ Ra	Fast Neutron (>0.18 Mev) $\times 10^{16}$ nvt	Exposure Time (min)
TNT	A11	1.8	2.1	25
	A13, A21	2.3	1.6	125
HMX/EXON	B12, B13, B14, B25	1.75	2	25
	B21, B22, B24, B26	0.61	0.7	8.7
DATB	C13, C14, C15	1.75	2.0	25
	C21, C22	8.95	10.5	125
	C23	4.35	4.3	125
PETN	D12, D13	1.75	1.7(1.9)	25
	D14, D22 D24	0.61	0.7(0.66)	8.7
	D21	1.75	0.77	25
	D25, D26	0.61(0.36)	0.22	8.7(9.34)

[a] References 1 and 2.

The grouping of samples according to dose level and exposure time was adopted when it was found that the infrared spectrum of each sample in a particular group was identical to the others. Verification of this may be found in the spectral data given in Tables 2 through 5.

Differential Thermal Analysis (DTA)

The DTA curves for each of the irradiated samples together with the standard explosives tested are shown in Figures 5 (a through d), 6 (a through i), 7 (a through i), and 8 (a through g). The data extracted from the DTA curve for each explosive is compiled in Table 6.

X-Ray Diffraction Analysis

Figures 9 through 12 show the x-ray diffractograms of irradiated samples A11, A21, B12, B22, C13, C21, C23, D12, D14, D21 and D25 and the corresponding explosive standards. Each irradiated sample x-ray diffractogram is, as explained under Infrared Spectrophotometric Analysis (directly above), representative of a group of samples having the same dose level and exposure time. A compilation of the x-ray diffraction data in terms of interplanar (d) spacing in Å units is given in Table 7.

Melting Point Determination

Melting point data for the irradiated samples, with the exception of the HMX/EXON, is given in Table 8. The melting points of the HMX/EXON samples were not determined since this determination is considered inapplicable to multi-component explosives.

Viscosity Measurements

Data obtained from the viscosity measurements of acetone solutions of irradiated propellants E11, F22 and G21 together with similar data for corresponding standards are given in Table 9.

Ultraviolet Spectrophotometric Examination

The ultraviolet spectra of irradiated nitrocellulose-base propellants E11 and F22 together with those of relevant standards are shown in Figure 13 (a through d).

DISCUSSION OF RESULTS

Effects of Irradiation

TNT (Trinitrotoluene)

The melting point and DTA data (Tables 6 and 8) together with a weight loss of less than one percent at both exposure levels (Table 10) indicate that TNT suffered only slight decomposition. The melting point was decreased about 5°C (max) at both exposure levels and the DTA curves show that the decomposition exotherm is decreased about 15°C, also at both exposure levels.

The infrared spectra of the TNT irradiated at the two dose levels reveal the presence of a small spectral band at around 810 cm^{-1}. Past work (Ref 5) with TNT irradiated with Co-60 (at 2.3×10^6 r/hr for 450 hours) showed that the 810 cm^{-1} band is due to a decomposition product, as yet unidentified. The Co-60 (γ) irradiated TNT melted in the range of 63° to 73°C (a maximum decrease of 17°) and its decomposition as determined by chromatographic analysis amounted to about 30%. In comparison, the TNT tested under this program did not suffer nearly as much radiation damage as did the Co-60 (γ) irradiated TNT. Supporting this conclusion is nondetection of solid crystalline decomposition products by x-ray diffraction analysis.

HMX/EXON (Cyclotetramethylenetetranitramine/EXON)

The HMX/EXON samples suffered weight losses of about 2% at low exposure and about 10% at high exposure levels (Table 10). Urizar (Ref 6) found the weight lost by HMX through nuclear reactor irradiation was essentially due to volatile decomposition products. The x-ray diffraction analysis supports this in that no solid decomposition products were detected.

The DTA curves (Fig 6b and 6i) exhibit an exotherm, common to all irradiated HMX/EXON samples but missing in the standard sample (6a), which begins at about 110°C and peaks at about 165-167°C. The exotherm was encountered by Urizar when HMX (minus EXON) was irradiated in a power reactor at integrated flux levels of approximately 10^{15} n/cm^2 (and 5×10^6R) and 3×10^{16} n/cm^2 (and 2×10^8R). Urizar was unable to explain this exotherm and tentatively concluded that it resulted from the annealing of stored energy. The endotherm at 202°C exhibited by the standard HMX/EXON

DTA curve is believed to be indicative of the $\beta \rightarrow \delta$ polymorphic transition of HMX. The low radiation dose shifted this endotherm to 186°C, and the high dose further decreased it to 182-185°C. The irradiation of the HMX/EXON shifted the decomposition temperature, exhibited by the exotherm at 308°C, to slightly lower temperatures at both exposure levels.

Infrared spectra indicated no change in HMX/EXON composition at the low exposure. The IR spectra of samples irradiated at the high dose, however, exhibited a very weak band at 1111-1113 cm^{-1}. This IR band is indicative of condensed decomposition products since solid decomposition products essentially are not formed during decomposition.

DATB (Diaminotrinitrobenzene)

At the low dose level the weight loss is about 2% while at the high dose level the loss amounted to about 6% (Table 10). The infrared spectra (Fig 3) for the irradiated DATB samples do not show any evidence of decomposition, nor does the x-ray diffraction data (Table 5) indicate any solid decomposition products. The melting point was decreased 1 to 2 degrees, depending on exposure time, suggesting slight decomposition. The melting point data is supported by the (melt) endotherm exhibited by the DTA curves (Figures 8a to 8g) for the irradiated DATB. In the latter analysis, the endotherm ordinarily at 294°C was decreased 2 to 4 degrees, depending on the dose level.

The DTA curve for standard DATB exhibits, in addition to the above-indicated melt endotherm, endotherms at 231°C and at 348°C. At low exposure, the endotherm at 231°C is shifted upward to an average temperature of 241°C where the one at 348° apparently is not affected by irradiation. At high exposure both endotherms are apparently missing. The significance of these changes is not understood at the present time.

An anomaly is found in the temperature region where the DTA decomposition exotherm of DATB occurs. Regardless of the level of exposure this exotherm appears at a higher temperature (see Table 6) instead of a lower temperature than the standard, as had been found with the other irradiated explosives.

PETN (Pentaerythritol tetranitrate)

The infrared, DTA, and melting point data show that the decomposition of PETN increases greatly with increasing

exposure. At very low exposure (0.2×10^{16} nvt fast neutrons, and 0.3×10^{8}R gamma radiation) PETN suffers a 3 degree decrease in melting point. Red fumes indicating NO_2 were detected during the melting point determination. The infrared spectra, at the low dose level, exhibit a very weak spectral band at a frequency of 2330 cm^{-1} (see Table 5). The DTA curves (Figures 7a to 7i), however, do not exhibit any differences in the endo- or exotherm temperatures.

At the intermediate exposure (0.7×10^{16} nvt fast neutrons and 0.6×10^{8}R gamma-irradiation), the melting point is decreased 7 degrees. The DTA curves exhibit a 4- to 7-degree downward shift of the small endotherm at 135°C, a decrease of 4 to 6 degrees in the melt endotherm and a lowering of 5 to 6 degrees in the peak value (extrapolated) of the decomposition exotherm. The DTA curves also exhibit a very small broad exotherm between 100° and 125°C, which may indicate an annealing effect or some exothermic chemical reaction taking place. Sample D24 is the only sample within this PETN group that does not show the small broad exotherm but instead exhibits a broad endotherm in the same temperature range. This behavior cannot be explained for the particular exposure conditions. The IR spectra of these samples are similar to those obtained for samples exposed to the low dose, except for D14, which shows a very weak spectral band at 2750 cm^{-1}. This band is also encountered in the spectra for samples exposed at the higher dose.

At higher exposure (1.9×10^{16} nvt fast neutrons, and 1.75×10^{8}R gamma radiation) PETN undergoes greater changes. The melting point is decreased by 7 to 13 degrees and the DTA exhibits a broad endotherm beginning at about 70°C and extending to about 140°C. The DTA for sample D12 shows the melt endotherm obscured by the broad endotherm. The decomposition endotherm, however, is not affected to any great extent (see Table 6). This broad endotherm may be indicative of some endothermic chemical reaction or physical change involving the products of decomposition. The products apparently are extensive, judging from the infrared spectra. Evidence for this is found in the appearance of spectral bands at frequencies of 1575 cm^{-1} and 1743 cm^{-1} and by a decrease in the 2750 cm^{-1} band. The 1743 cm^{-1} band is indicative of the carbonyl group and the 1575 cm^{-1} band indicative of the nitroso group. No evidence of impurities is shown by x-ray diffractograms (Fig 12), indicating that most of the impurities found are noncrystalline.

Propellants

Viscosity data (Table 9) and ultraviolet spectra (Figure 13a through d) indicate that the nitrocellulose-base propellants (samples E11, F22, and G21) are decomposed by reactor radiation. The large difference in viscosity values between the standard and the irradiated propellant is indicative of a gross breakdown of the nitrocellulose molecule. Further evidence is obtained from the ultraviolet spectra for irradiated M-6 and T-28, which show an increase in the absorbancy in the 260-390 mμ range. The large absorbance is due to the nitrated stabilizer and indirectly shows the depletion of the stabilizer content. The nitrocellulose, upon depletion of the stabilizer, is no longer stabilized, and therefore it is allowed to continue to decompose unchecked. This acceleration of the decomposition of nitrocellulose by nuclear reactor irradiation has been reported by Urizar, et al. (Ref 6).

Chemical Stability

A summary of the data for each irradiated explosive according to exposure level is given in Table 10. The data for the propellants (nitrocellulose base) is discussed under Effects of Irradiation.

The relative order of chemical stability of the four explosives under irradiation is based on a common exposure level. This level is found in the fast neutron exposure of 2.0×10^{16} nvt and gamma exposure of 1.8×10^{8}R. At this level, DATB is the most stable of the four explosives. It exhibits the smallest decrease in melting point, absence of decomposition as shown by the infrared spectra, and a small percentage weight loss. Further evidence of DATB's relative chemical stability under irradiation is shown by the magnitude of change induced at the higher dose level (10.5×10^{16} nvt, fast neutrons and 8.75×10^{8}R, gamma) or less than the changes exhibited by the other three explosives at the lower dose level (see Table 10).

The large percentage weight loss (Ref 1) exhibited by HMX/EXON would indicate that it is less stable than TNT (Table 10). The mechanism of decomposition for each explosive is not known but it appears that the decomposition products produced by HMX are mostly in the form of volatiles. When TNT decomposes, it produces considerably more solid decomposition products, which would result in a low percentage weight loss. The data as a whole, however, indicates

that HMX/EXON is slightly more stable to irradiation than TNT or PETN.

Of the two remaining explosives, TNT is apparently more stable than PETN. The large decrease in melting point, the high percentage weight loss (Table 10), and the relatively major changes exhibited by PETN, as indicated by infrared spectra, are evidence of its relative chemical instability at the common exposure level. At a lower dose level (Table 10), PETN still appears to be less stable than HMX/EXON. Even at the very low fast neutron exposure of 0.22×10^{16} nvt and gamma exposure of 0.48×10^{8}R (average), the infrared spectra still indicates PETN undergoes slight changes.

The effect of irradiation on the nitrocellulose-base propellants has been discussed earlier.

From the data obtained, it is obvious that the nitrocellulose-base propellants undergo major changes during the irradiation. These propellants, therefore, have a relatively low order of chemical stability under nuclear reactor irradiation.

ACKNOWLEDGEMENTS

The viscosity measurements and ultraviolet spectra for the propellant were obtained from Mr. M. Halik of the Propellants Laboratory The x-ray diffractograms for the explosives and pertinent information were obtained from Mr. J. J. Campisi, also of the Propellants Laboratory. The differential thermal analyses curves were obtained from Mr. C. Campbell of the Pyrotechnics Laboratory, all at Picatinny. We thank all these people for their cooperation and advice in making possible these analyses.

REFERENCES

1. Aerojet General Corporation (Sacramento, California), Report RN-S-0210, April 1965

2. General Electric Company, Santa Barbara, California, "The Effects of Reactor Radiations on the Impact Sensitivity of Explosive Solids," Report #RM 64 TMP-45, 1964

3. Saul Gordon and Clement Campbell, "Differential Thermal Analysis of Inorganic Compounds," Analytical Chemistry 27 p. 1102, July 1955

4. Propellant Laboratory Report No. 64-VG1-82 (Picatinny Arsenal, Dover, N.J., 1964

5. C. Ribaudo, Unpublished work

6. M. J. Urizar, E. D. Loughran, and L. C. Smith, "The Effects of Nuclear Radiation on Organic Explosives," Explosivstoffe 10:3, pp 55-64, 1962

TABLE 1

Material irradiated in a high flux test reactor

Material	Sample No.	Approximate Amount Shipped, g	Exposure (Neutron E>0.18 Mev, 10^{16} nvt)	Decay Time, Days[a]	Activity (β+γ), nc/g
TNT (trinitrotoluene 2,4,6)	A11	1.0	2.1	100	0.023
	A13	0.7	1.6		
	A21	1.7	1.5		
HMX/EXON 2[b] (95% cyclotetramethylenetetranitramine 5% EXON)	B12	0.1	2.0		
	B13	0.3	2.2		
	B14	1.7	2.0		
	B21	0.3	0.78		
	B22	1.7	0.73		
	B24	0.4	0.74		
	B25	0.4	2.3	69	1.6
	B26	0.4	0.77		
DATB (diaminotrinitrobenzene)	C13	0.3	2.2		
	C14	0.3	1.9		
	C15	1.5	2.0		
	C21	0.4	10.5		
	C22	0.5	10.5		
	C23	1.6	4.3	68	0.13
PETN (pentaerythritol tetranitrate	D12	0.1	1.7	68	0.13
	D13	0.2	1.9		
	D14	0.6	0.77		
	D21	1.7	0.77		
	D22	0.4	-		
	D24	0.7	0.66	69	0.0049
	D25	1.7	0.24		
	D26	0.8	0.21		
M-6 Propellant[c]	E11	0.3	0.95	67	0.0052
T-28 Propellant[c]	F22	0.2	0.40	67	0.011
T-36 Propellant[c]	G21	0.2	0.43	67	0.021

[a] The decay time is number of days between irradiation date and date shipped to Picatinny (the date activity measurements were made).

[b] HMX/EXON - 5% by weight EXON 461 (chlorofluoropolymer) binder.

[c] See Reference 1 for propellant compositions.

TABLE 2

Infrared spectral data
for irradiated TNT
(frequency in cm^{-1})

Capsule:	Standard	A11	A13	A21
Gamma-ray exposure ($x10^8$R)	-	1.8	2.3	2.3
Fast neutron flux, >0.18 Mev ($x10^{16}$ nvt)	-	2.1	1.6	1.5
Exposure time (Minutes)	-	25	125	125
	1608(M)	1605(M)	1608(M)	1608(M)
	1538(VS)	1535(VS)	1538(VS)	1538(VS)
	1463(W)	1467(W)	1463(W)	1463(W)
	1438(W)	1439(W)	1438(W)	1438(W)
	1402(W)	1403(W)	1402(W)	1402(W)
	1350(VS)	1352(VS)	1350(VS)	1350(VS)
	1205(W)	1203(W)	1205(W)	1205(W)
	1170(W)	1168(W)	1170(W)	1170(W)
	1085(M)	1085(M)	1085(M)	1085(M)
	1025(W)	1025(W)	1025(W)	1025(W)
	938(M)	938(M)	938(M)	938(M)
	907(S)	906(s)	907(S)	907(S)
	824(W)	823(W)	824(W)	824(W)
		808(W)	810(W)	810(W)
	792(M)	792(M)	792(M)	792(M)
	767(W)	767(W)	767(W)	767(W)
	758(W)	758(W)	758(W)	758(W)
	734(M)	734(M)	734(M)	734(M)
	717(S)	717(S)	717(S)	717(S)
	703(W)	703(W)	703(W)	703(W)

VS = very strong band
S = strong band
M = medium band
W = weak band

TABLE 3

Infrared spectral data for irradiated HMX/EXON (frequency in cm^{-1})

Capsule:	Standard	B12	B13	B14	B25	B21	B22	B24	B26
Gamma-ray exposure ($\times 10^8$ R)		1.75	1.75	1.75	1.75	0.61	0.61	0.61	0.61
Fast neutron flux, >0.18 Mev ($\times 10^{16}$ nvt)		2.0	2.2	2.0	2.3	0.78	0.73	0.74	0.77
Exposure time (Minutes)		25	25	25	25	8.7	8.7	8.7	8.7
	3070 (W)	3070 (W)	3040 (W)	3030 (W)	3030 (W)	3030 (W)	3030 (W)	3030 (W)	3030 (W)
	1575 (VS)	1575 (VS)	1575 (VS)	1575 (VS)	1575 (VS)	1575 (VS)	1575 (VS)	1575 (VS)	1575 (VS)
	1470 (M)	1470 (M)	1468 (M)	1465 (M)	1465 (M)	1465 (M)	1465 (M)	1465 (M)	1465 (M)
	1440 (M)	1440 (M)	1438 (M)	1435 (M)	1435 (M)	1435 (M)	1435 (M)	1435 (M)	1435 (M)
	1405 (M)	1405 (M)	1400 (M)	1400 (M)	1400 (M)	1400 (M)	1400 (M)	1400 (M)	1400 (M)
	1353 (W)	1353 (W)	1350 (W)	1348 (W)	1348 (W)	1348 (W)	1348 (W)	1348 (W)	1348 (W)
	1287 (VS)	1287 (VS)	1287 (VS)	1287 (VS)	1287 (VS)	1287 (VS)	1287 (S)	1287 (S)	1287 (S)
	1242 (VW)	1242 (VW)	1240 (W)	1238 (VW)	1238 (VW)	1238 (VW)	1238 (VW)	1238 (VW)	1238 (VW)
	1205 (M)	1205 (M)	1203 (M)	1203 (M)	1203 (M)	1203 (M)	1203 (M)	1203 (M)	1203 (M)
	1149 (M)	1149 (M)	1146 (M)	1146 (M)	1146 (M)	1146 (M)	1146 (M)	1146 (M)	1146 (M)
		1113 (WW)	1112 (VVW)	1111 (WW)	1111 (VVW)				
	1090 (M)	1090 (M)	1087 (M)	1087 (M)	1087 (M)	1087 (M)	1087 (M)	1087 (M)	1087 (M)
	967 (S)	967 (S)	967 (S)	967 (S)	967 (S)	967 (S)	967 (S)	967 (S)	967 (S)
	945 (S)	945 (S)	945 (S)	945 (S)	945 (S)	945 (S)	945 (S)	945 (S)	945 (S)
	918 (VVW)	918 (VVW)	918 (VVW)	918 (VVW)	918 (VVW)	918 (VVW)	918 (VVW)	918 (VVW)	918 (VVW)
	872 (W)	873 (W)	873 (W)	872 (W)	872 (W)	872 (W)	872 (W)	872 (W)	872 (W)
	831 (M)	831 (M)	831 (M)	830 (M)	830 (M)	830 (M)	830 (M)	830 (M)	830 (M)
	772 (W)	772 (W)	772 (W)	770 (W)	770 (W)	770 (W)	770 (W)	770 (W)	770 (W)
	762 (M)	762 (M)	761 (M)	760 (M)	760 (M)	760 (M)	763 (M)	760 (M)	760 (M)

VS = very strong band
M = medium band
W = weak band
VW = very weak band
VVW = very very weak band

TABLE 4

Infrared spectral data for irradiated DATB (frequency in cm^{-1})

Capsule:	Standard	C21	C22	C23	C13	C14	C15
Gamma-ray exposure ($\times 10^8$ R)		8.95	8.95	4.35	1.75	1.75	1.75
Fast neutron flux, >0.18 Mev ($\times 10^{16}$ nvt)		10.5	10.5	4.3	2.2	1.9	2.0
Exposure time (minutes)		125	125	125	25	25	25
	3380 (M)	3380 (W)	3380 (M)	3380 (M)	3380 (M)	3380 (M)	3380 (M)
	3280 (M)	3280 (M)	3280 (M)	3280 (M)	3280 (M)	3280 (M)	3280 (M)
	1608 (S)	1608 (S)	1608 (S)	1608 (S)	1608 (S)	1608 (S)	1608 (S)
	1562 (W)	1558 (W)	1562 (W)	1558 (W)	1558 (W)	1560 (W)	1562 (W)
	1525 (W)	1526 (W)	1527 (W)	1525 (W)	1525 (W)	1525 (W)	1527 (W)
	1475 (W)	1480 (W)	1475 (W)	1475 (W)	1475 (W)	1475 (W)	1475 (W)
	1452 (VW)	1452 (VW)	1452 (VW)	1452 (VW)	1452 (VW)	1452 (W)	1452 (W)
	1365 (M)	1367 (M)	1366 (M)	1368 (M)	1365 (M)	1365 (M)	1366 (M)
	1305 (M)	1305 (M)	1304 (M)	1304 (M)	1305 (M)	1305 (M)	1304 (M)
	1225 (S)	1225 (S)	1225 (S)	1225 (S)	1225 (S)	1225 (S)	1225 (S)
	1152 (VVW)	1152 (VVW)	1155 (VVW)	1152 (VVW)	1152 (VVW)	1152 (VVW)	1155 (VW)
	1028 (M)	1032 (M)	1032 (M)	1032 (M)	1028 (M)	1030 (M)	1032 (M)
	945 (W)	948 (W)	947 (VW)	947 (W)	947 (W)	947 (W)	947 (W)
	905 (W)	905 (W)	905 (W)	903 (W)	905 (W)	903 (W)	905 (W)
	888 (M)	889) M)	889 (M)	889 (W)	888 (M)	889 (M)	889 (M)
	828 (W)	830 (W)	830 (W)	830 (W)	828 (W)	830 (W)	830 (W)
	778 (M)	780 (M)	782 (M)	780 (M)	778 (M)	780 (M)	782 (M)
	754 (W)	756 (W)	757 (W)	754 (W)	754 (W)	754 (W)	757 (VW)
	727 (W)	727 (W)	727 (W)	727 (W)	727 (W)	727 (W)	727 (W)
	703 (W)	703 (W)	702 (W)	702 (VW)	703 (W)	702 (W)	702 (W)
	673 (W)	675 (W)	675 (W)	675 (W)	673 (W)	675 (W)	675 (W)

S = strong band
M = medium band
W = weak band
VW = very weak band
VVW = very very weak band

TABLE 5

Infrared spectral data
for irradiated PETN
(frequency in cm^{-1})

Capsule:	Standard	D12	D13	D21	D14	D22	D24	D25	D26
Gamma-ray exposure ($\times 10^8$ R)	-	1.75	1.75	1.75	0.61	0.61	0.61	0.61(?)	0.36
Fast neutron flux, >0.18 Mev ($\times 10^{16}$ nvt)		1.7	1.9	0.77	0.77	-	0.66	0.24	0.22
Exposure time (minutes)	-	25	25	25	8.7	8.7	8.7	8.7	9.34
	2925(VW)	2925(W)	2925(W)	2925(W)	2925(W)	2925(W)	2925(W)	2925(W)	2925(W)
	2750(VW)	-	-	-	-	2750(VW)	2750(VW)	2750(VW)	2750(VW)
	2650(VW)	2650(VW)	2650(VW)	2650(VW)	2650(VW)	2650(VW)	2650(VW)	2650(VW)	2650(VW)
	2550(VW)	2550(VW)	2550(VW)	2550(VW)	2550(VW)	2550(VW)	2550(VW)	2550(VW)	2550(VW)
	-	2330(W)	2330(W)	2330(W)	2330(W)	2330(W)	2330(W)	2330(W)	2330(W)
	-	2230(VVW)	2230(VVW)	2230(VVW)	2230(VVW)	2230(VVW)	2230(VVW)	2230(VVW)	2230(VVW)
	-	1743(VW)	1743(VW)	1743(VW)	-	-	-	-	-
	1653(S)	1653(S)	1653(S)	1653(S)	1653(S)	1653(S)	1653(S)	1653(S)	1653(S)
	-	1575(VW)	1575(VVW)	1575(W)	-	-	-	-	-
	1505(VW)	1505(VW)	1505(VW)	1503(VW)	1510(VW)	1505(VW)	1505(VW)	1505(VW)	1505(VW)
	1475(M)	1475(M)	1475(M)	1470(M)	1470(M)	1470(M)	1470(M)	1470(M)	1470(M)
	1392(M)	1392(M)	1392(M)	1395(M)	1395(M)	1395(M)	1395(M)	1395(M)	1395(M)
	1305(W)	1305(W)	1305(W)	1305(W)	1305(W)	1305(W)	1305(W)	1305(W)	1305(W)
	1283(S)	1283(S)	1283(S)	1282(S)	1282(S)	1282(S)	1282(S)	1282(S)	1282(S)
	1192(VW)	1192(VW)	1192(VW)	1192(VW)	1192(VW)	1192(VW)	1192(VW)	1192(VW)	1192(VW)
	1158(VW)	1158(VW)	1158(VW)	1156(VW)	1156(VW)	1156(VW)	1156(VW)	1156(VW)	1156(VW)
	1037(M)	1037(M)	1037(M)	1037(M)	1037(M)	1037(M)	1037(M)	1037(M)	1037(M)
	1000(M)	1000(M)	1000(M)	1000(M)	1000(M)	1000(M)	1000(M)	1000(M)	1000(M)
	938(M)	938(M)	939(M)	937(M)	937(M)	937(M)	937(M)	937(M)	937(M)
	867(M)	867(M)	867(M)	867(M)	867(M)	867(M)	867(M)	867(M)	867(M)
	847(VS)	847(VS)	847(VS)	847(VS)	847(VS)	847(VS)	847(VS)	847(VS)	847(VS)
	753(M)	753(M)	753(M)	753(M)	753(M)	753(M)	753(M)	753(M)	753(M)
	744(W)	744(W)	744(W)	744(W)	743(W)	743(W)	743(W)	743(W)	744(W)
	701(M)	701(M)	701(M)	702(M)	702(M)	702(M)	702(M)	702(M)	702(M)

VS = very strong bands
S = strong bands
M = medium bands
W = weak bands
VW = very weak bands
VVW = very very weak bands

TABLE 6

Differential thermal analysis data
for irradiated
TNT, HMX/EXON, DATB and PETN

Gamma-ray Exposure, 10^8 R	Fast Neutron Exposure, >0.18 Mev, 10^{16} nvt	Exposure Time, minutes	Capsule	Endotherms, °C			Exotherms °C	
				First	Second	Third	First	Second
-	-	-	Std TNT	80.7	-	-	346	
1.8	2.1	25	A11	79.0	-	-	329	
2.3	1.5	125	A13	79.0	-	-	336	
2.3	1.5	125	A21	77.0	-	-	331	
-	-	-	Std HMX/EXON	102(B)[a]	202	-	-	308
1.75	2.0	25	B12	-	185	-	165(B)	298
1.75	2.2	25	B13	-	182	-	167(B)	298
1.75	2.0	25	B14	-	182	-	167(B)	300
1.75	2.3	25	B25	-	185	-	165(B)	302
0.61	0.78	8.7	B21	-	186	-	165(B)	304
0.61	0.73	8.7	B22	-	186	-	165(B)	304
0.61	0.74	8.7	B24	-	186	-	165(B)	302
0.61	0.77	8.7	B26	-	186	-	165(B)	300
-	-	-	Std DATB	231	294	348	365	-
8.95	10.5	125	C21	-	290	-	373	-
8.95	10.5	125	C22	-	290	-	375	-
4.35	4.3	125	C23	-	290	-	382	-
1.75	2.2	25	C13	240	294	350	385	-
1.75	1.9	25	C14	242	292	349	375	-
1.75	2.0	25	C15	242	292	346	369	-
-	-	-	Std PETN	135	146	-	233	-
1.75	1.7	25	D12	-	-	-	226	-
1.75	1.9	25	D13	-	137	-	227	-
1.75	0.77	25	D21	128	138	-	227	-
0.61	0.77	8.7	D14	131	142	-	227	-
0.61	-	8.7	D22	131	141	-	228	-
0.61	0.66	8.7	D24	-	142	-	228	-
0.61	0.24	8.7	D25	135	146	-	233	-
0.36	0.22	9.34	D26	135	146	-	234	-

[a] B = broad

TABLE 7

X-ray diffraction data
for irradiated explosives
interplanar spacings in Å

Standard TNT	Capsules A11 & A21	Standard HMX/EXON	Capsules B12 & B22	Standard DATB	Capsules C13, C21 C23	Standard PETN	Capsules D12, D14, D21 & D25
7.02(S)	Inter-	6.06(S-)		7.34(VVS)		6.70(M)	
6.42(F)	planar	5.55(S-)	Interplanar	5.86(M+)	Interplanar	4.72(M)	Interplanar
6.03(W)	Spacings	4.87(W)	spacings	5.18(W)	spacings	4.23(M-)	spacings
5.65(S-)	identical	4.35(VVS)	identical	4.87(M-)	identical	3.86(VVS)	identical
5.47(W)	to	4.04(F)	to	4.34(S)	to	3.57(VS)	to
5.21(F)	standard	3.88(S)	standard	4.23(M-)	standard	3.32(S)	standard
5.00(S-)	TNT	3.42(M+)	HMX/EXON	4.07(M+)	DATB	3.16(M-)	PETN
4.61(F-)		3.29(M+)		3.89(M+)		2.98(M+)	
4.29(S)		3.21(W)		3.64(M)		2.85(M)	
4.11(F)		3.07(M)		3.53(S)		2.73(M)	
4.01(W)		3.02(M+)		3.29(M)		2.62(M)	
3.86(VVS)		2.95(VF)		2.96(VS)		2.37(M-)	
3.74(M)		2.81(VS)		2.84(W)		2.07(M-)	
3.53(M+)		2.70(F)		2.78(F)		1.89(F)	
3.45(M+)		2.55(F)		2.56(W)		1.82(M-)	
3.35(F)		2.42(M-)		2.49(W)		1.78(W)	
3.26(M+)		2.27(F)		2.21(M-)			
3.15(F)		2.20(M-)		2.16(M)			
3.06(S)		2.13(F)		2.13(M-)			
3.01(S-)		2.10(F)		2.00(W)			
2.93(F)		2.01(F)		1.84(W)			
2.87(M+)							
2.78(F)							
2.73(S-)							
2.67(S-)							
2.59(M)							
2.52(F)							
2.43(M+)							
2.36(M)							
2.30(M+)							
2.22(F)							

VVS = very very strong
VS = very strong
S = strong
M = medium
F = faint
VF = very faint

TABLE 8

Melting point data for irradiated
TNT, DATB & PETN

Exposure Time (minutes)	Capsule	Melting Point range, °C	Remarks
	Standard TNT	79.5 - 80.3	
25	A11	74 - 77	Decomposition gases not observed
125	A13	74 - 77.5	Decomposition gases not observed
125	A21	74 - 77.5	Decomposition gases not observed
	Standard DATB	281 - 283	Melting with decomposition
125	C21	279 - 281	Melting with decomposition
125	C22	279 - 281	Melting with decomposition
125	C23	280 - 281	Melting with decomposition
25	C13	280 - 283	Melting with decomposition
25	C14	280 - 283	Melting with decomposition
25	C15	280 - 282	Melting with decomposition
	Standard PETN	140.5 - 141.5	
25	D12	133 - 136	Decomposition with gas evolution
25	D13	128 - 132	Decomposition with gas evolution, some liquid noted
25	D21	133 - 137	Decomposition during melting, complete melt at 137°C
8.7	D14	133 - 136.5	Decomposition during melting, complete melt at 136.5°C
8.7	D22	133 - 136	Decomposition during melting, complete melt at 136°C
8.7	D24	134.5 - 137	Decomposition during melting, complete melt at 137°C
8.7	D25	137 - 139.5	Decomposition during melting, yellow decomposition gas
9.34	D26	137 - 139.5	Decomposition during melting, oxide of nitrogen detected

TABLE 9

Propellant viscosities

Sample	Viscosity
Capsule E-11	1.019
Standard M-6	1.789
Capsule F-22	1.101
Standard T-28	2.037
Capsule G-21	1.072
Standard T-36	1.523

TABLE 10

Summary of analytical data obtained for irradiated explosives

	Exposure Time, minutes	Fast Neutron Flux $\times 10^{16}$ nvt	γ-ray Dose $\times 10^{8}$ R	MP ΔT, °C	DTA[a] Endotherm, ΔT°C	DTA[a] Exotherm, ΔT°C	Weight Loss (Ref 2), %	Remarks
DATB	125	10.5	8.95	-4	-4	+9	0.73	IR and X-ray, no change detected
DATB	25	2.0	1.75	-2	-3	+12	0.15	IR and X-ray, no change detected
TNT	25	2.1	1.8	-5.7	-1.7	-17	0.92	IR detected change, X-ray no change
PETN	25	1.8	1.75	-10	-9	-7	10.53	IR detected change (major), X-ray no change
HMX/EXON	25	2.1	1.75	--	-18[b]	-9	10.42	IR detects change (slight), X-ray no change
HMX/EXON	8.7	0.72	0.61	--	-16[b]	-5	2.30	IR and X-ray, no change detected
PETN	8.7	0.76	0.61	-6	-5	-5	3.64	IR change detected, X-ray no change
PETN	9.34	0.23	0.48 (Av)	-3.5	0	0	--	IR change detected, X-ray no change

[a] Where ΔT indicates a shift in the sample temperature at which the exotherm or endotherm occurs; the positive direction is toward higher temperatures.

[b] $\beta \rightarrow \delta$ transition temperature.

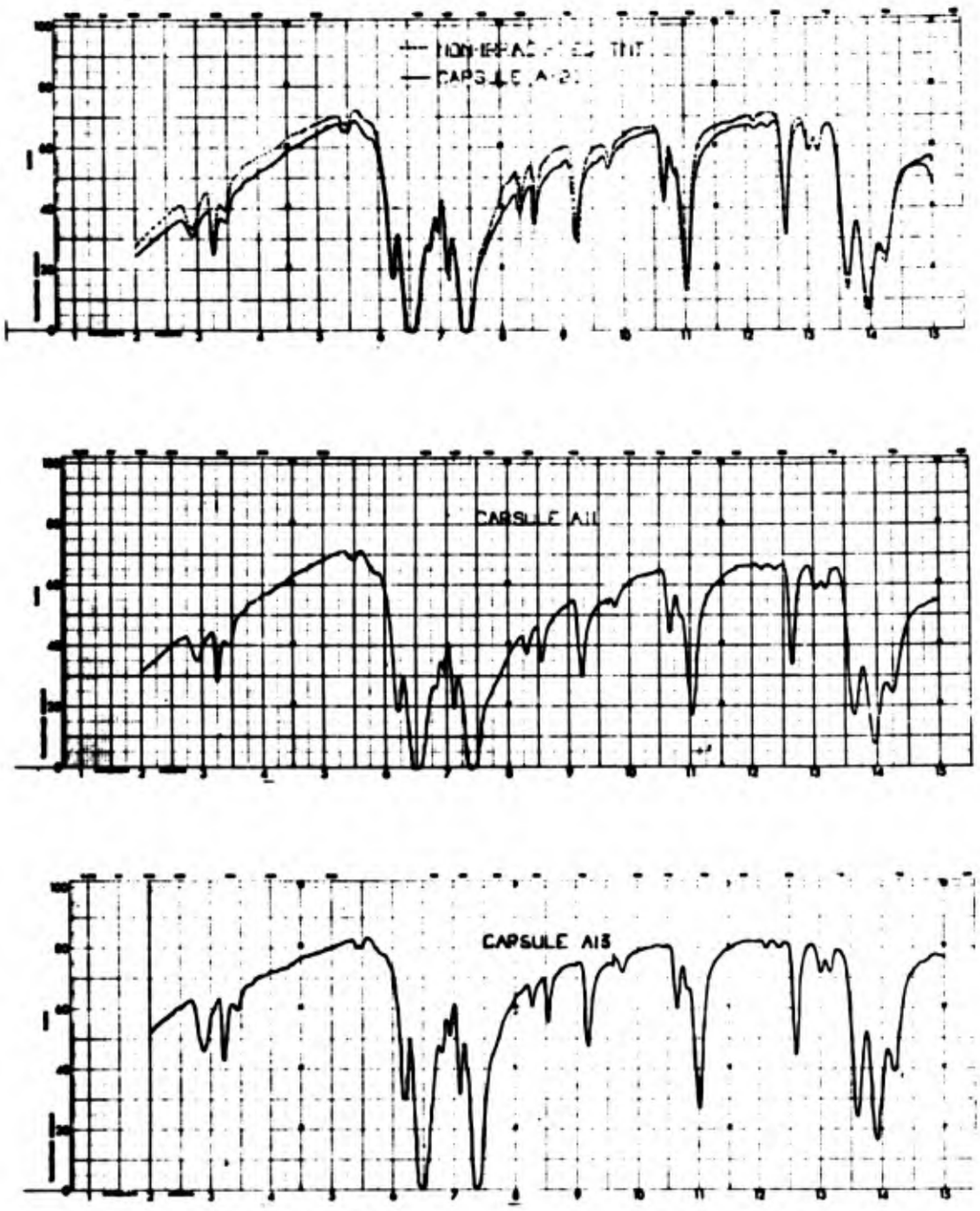

Fig 1 Infrared spectra for irradiated and standard TNT

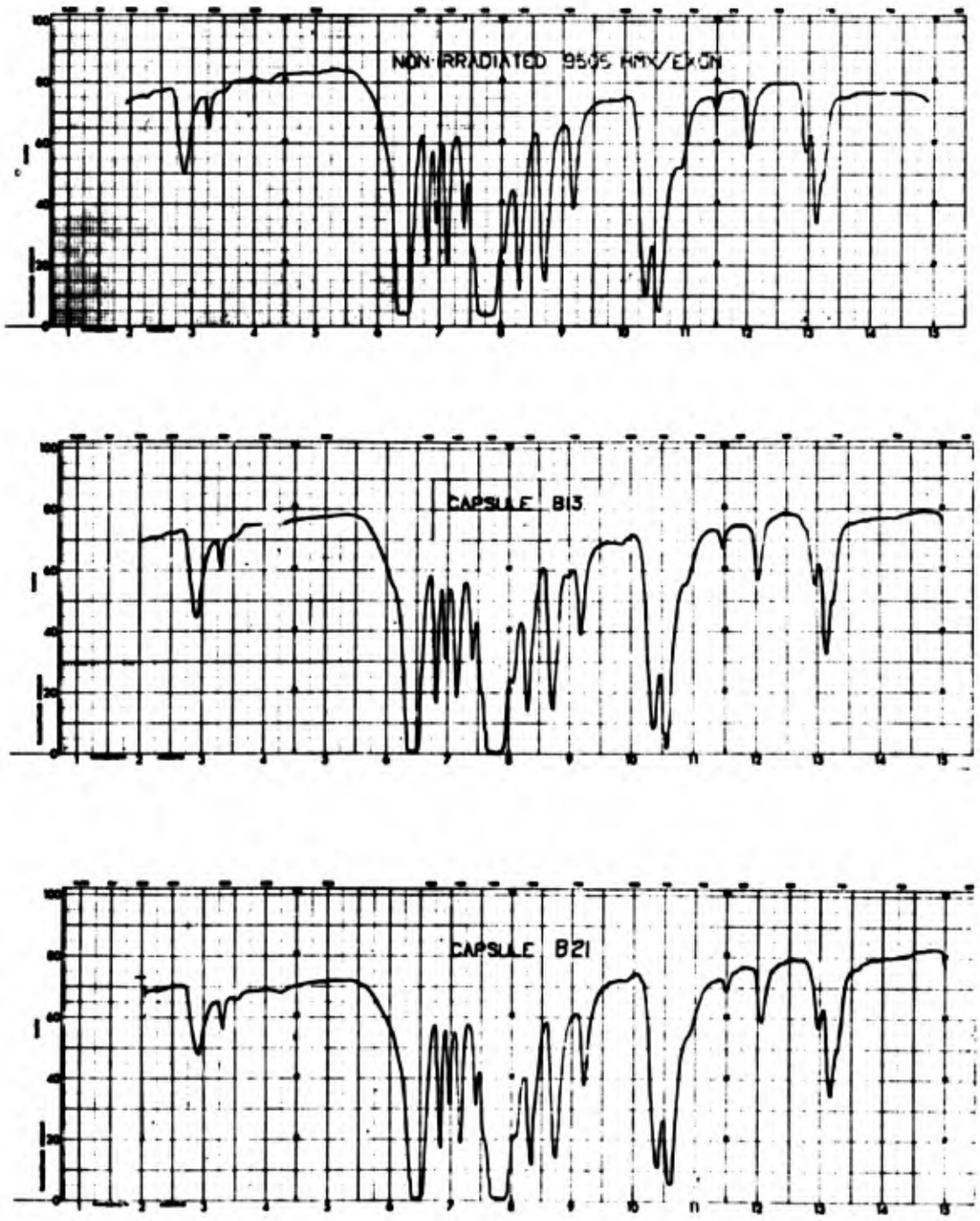

Fig 2 Infrared spectra for irradiated and standard HMX/EXON (9505)

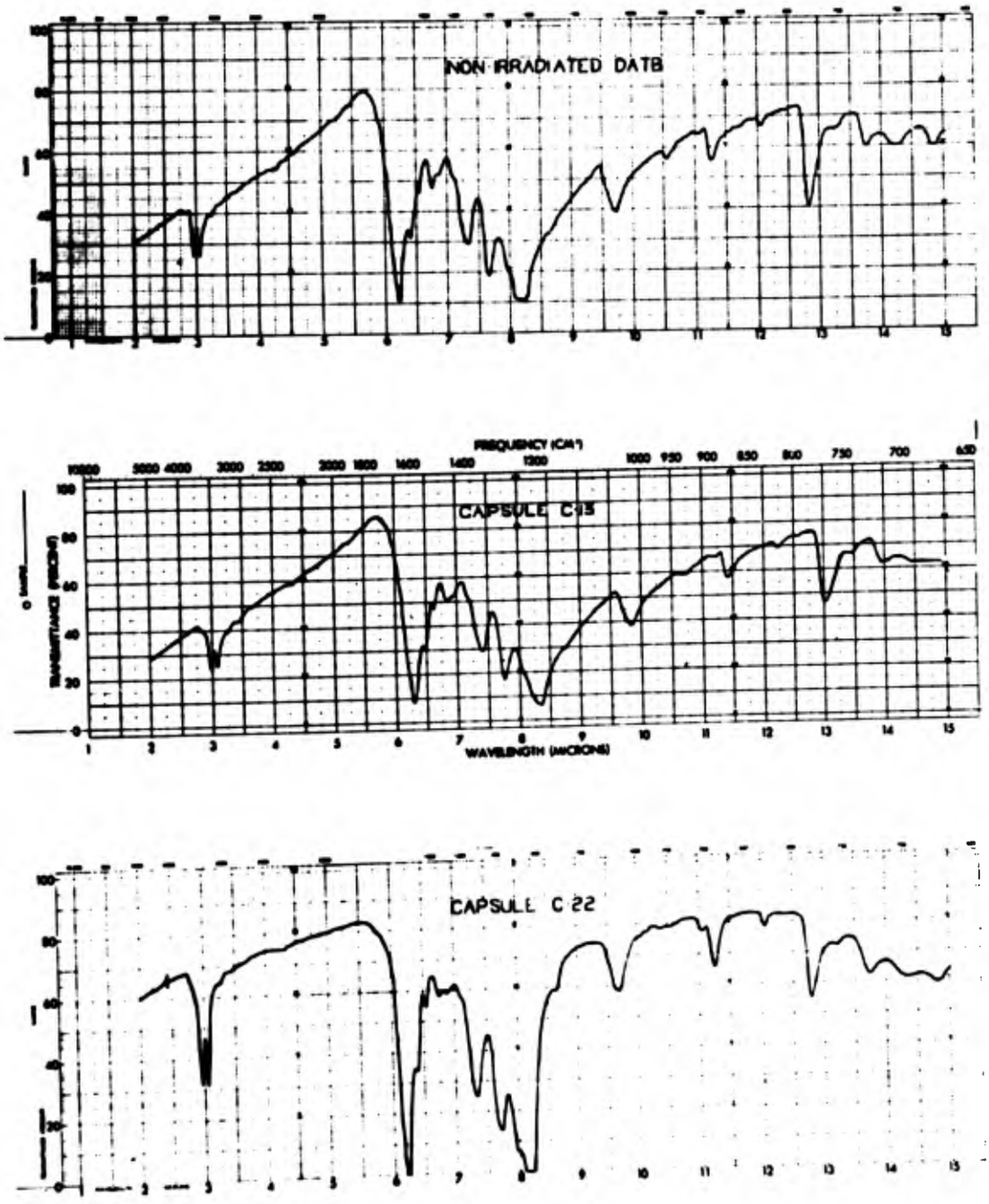

Fig 3 Infrared spectra for irradiated and standard DATB

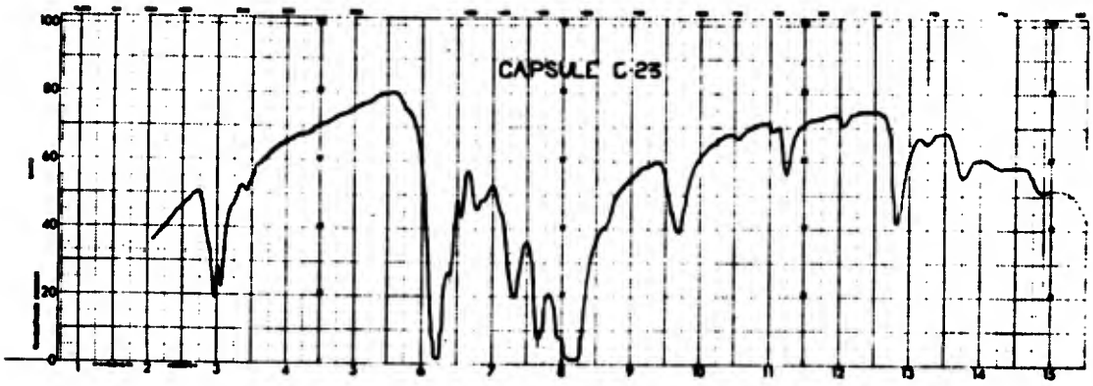

Fig 3 (cont) Infrared spectra for irradiated and standard DATB

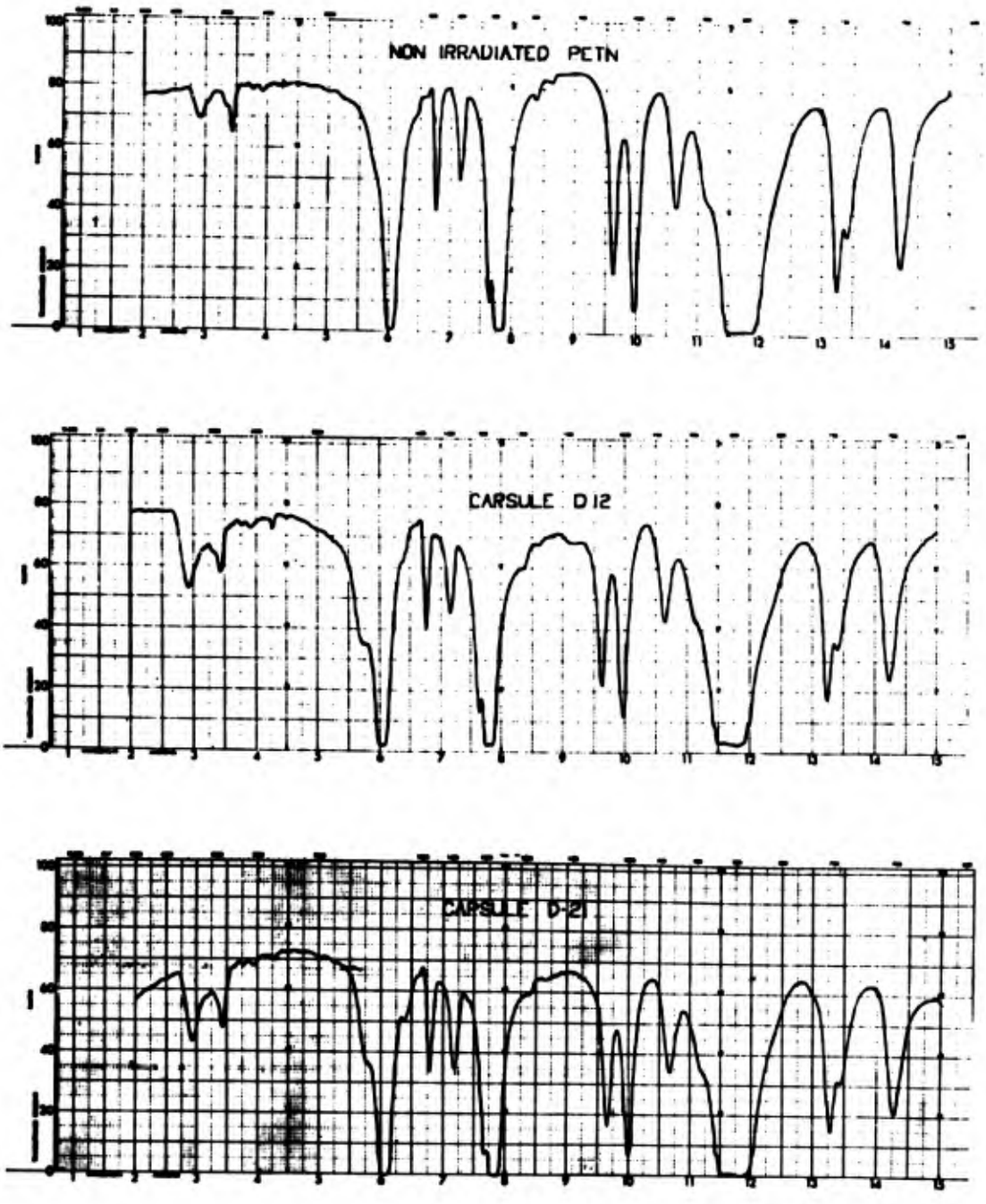

Fig 4 Infrared spectra for irradiated and standard PETN

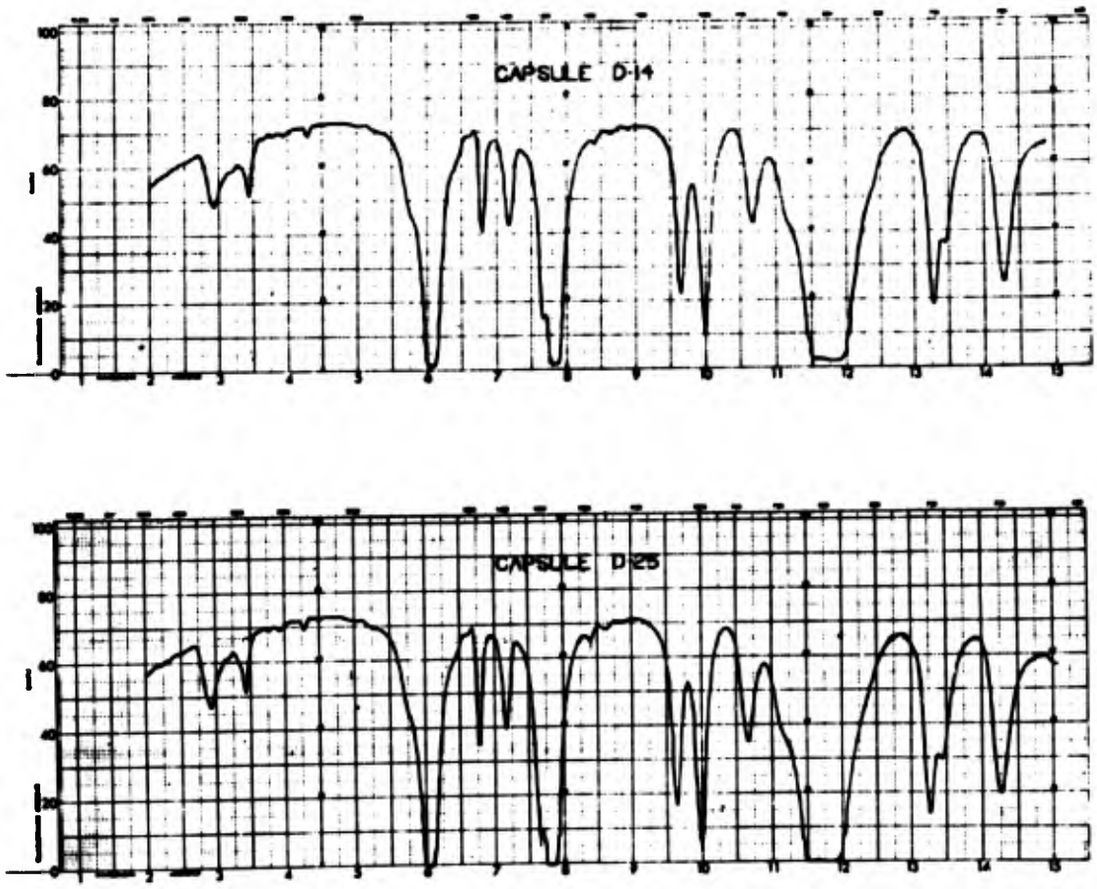

Fig 4 (cont) Infrared spectra for irradiated and standard PETN

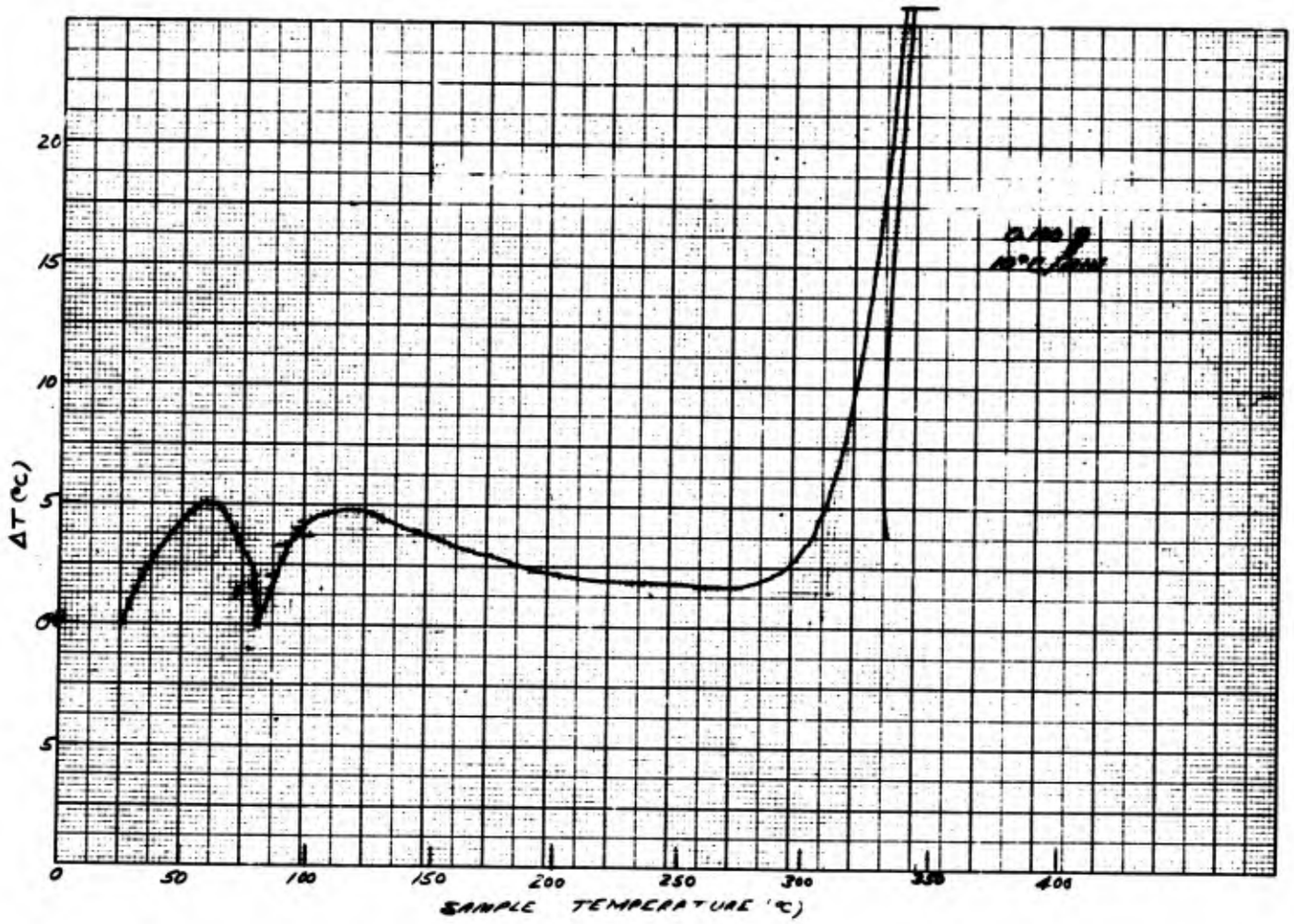

Fig 5a DTA curve for standard TNT

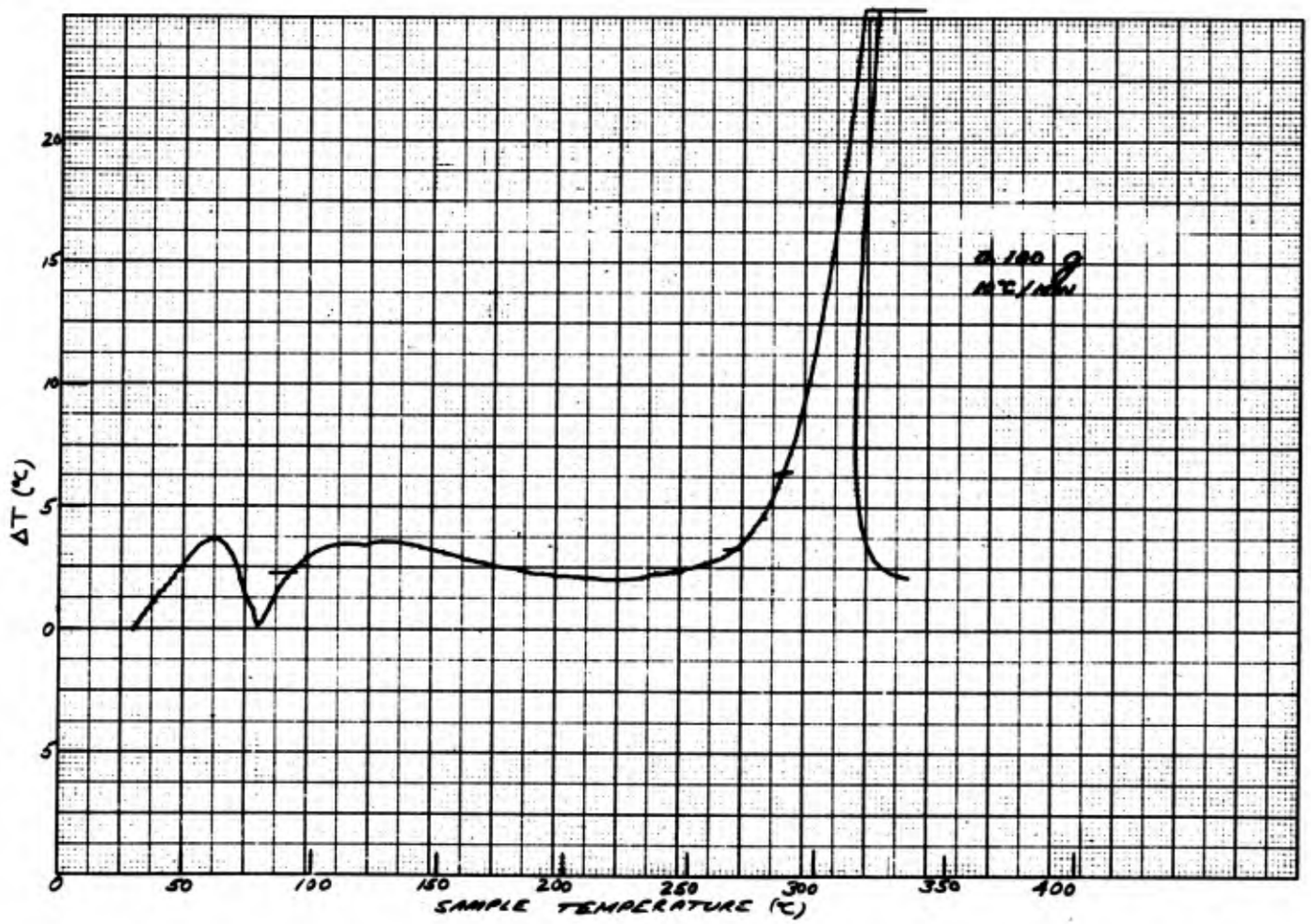

Fig 5b DTA curve for irradiated TNT, Sample A11

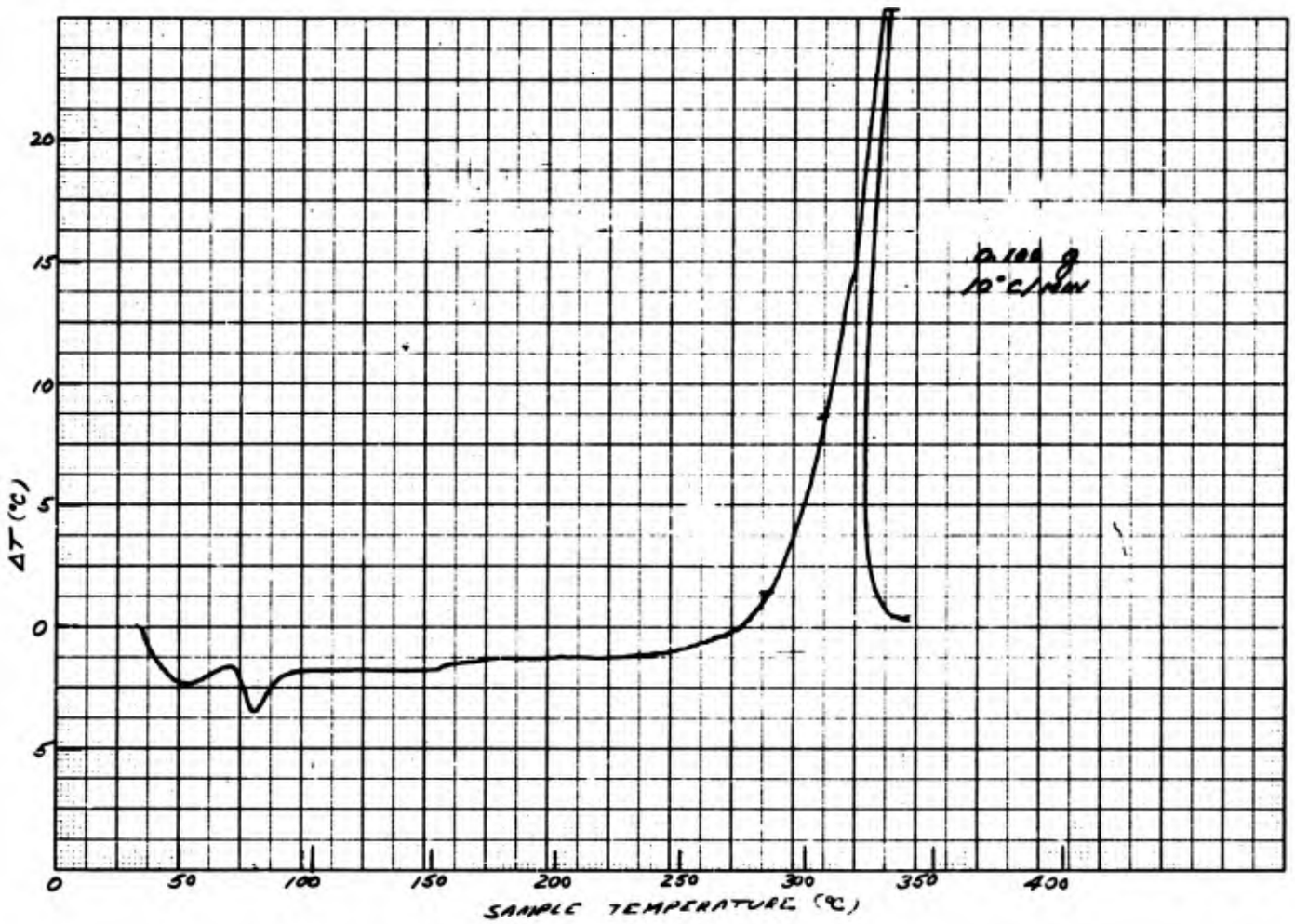

Fig 5c DTA curve for irradiated TNT, Sample A13

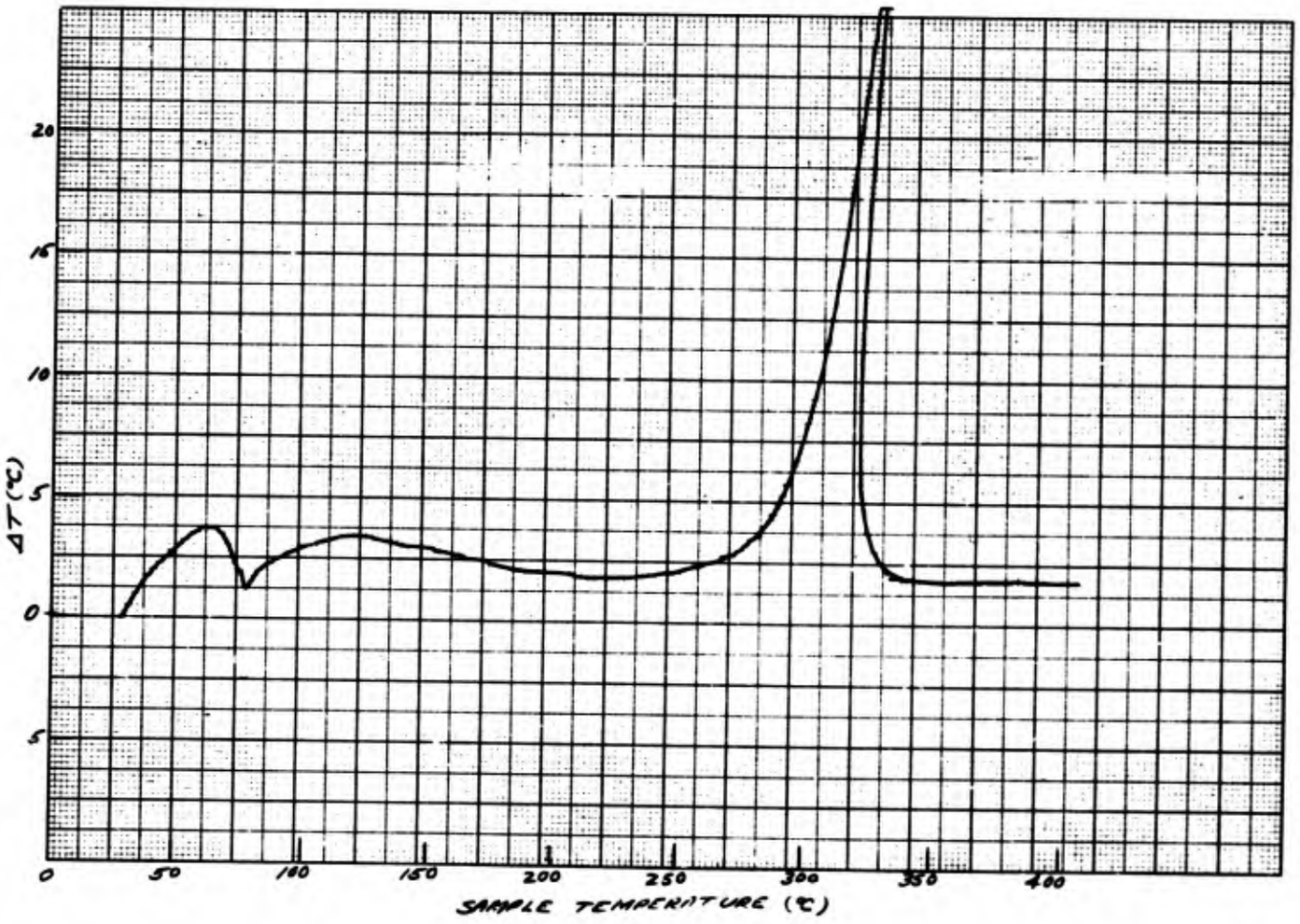

Fig 5d DTA curve for irradiated TNT, Sample A21

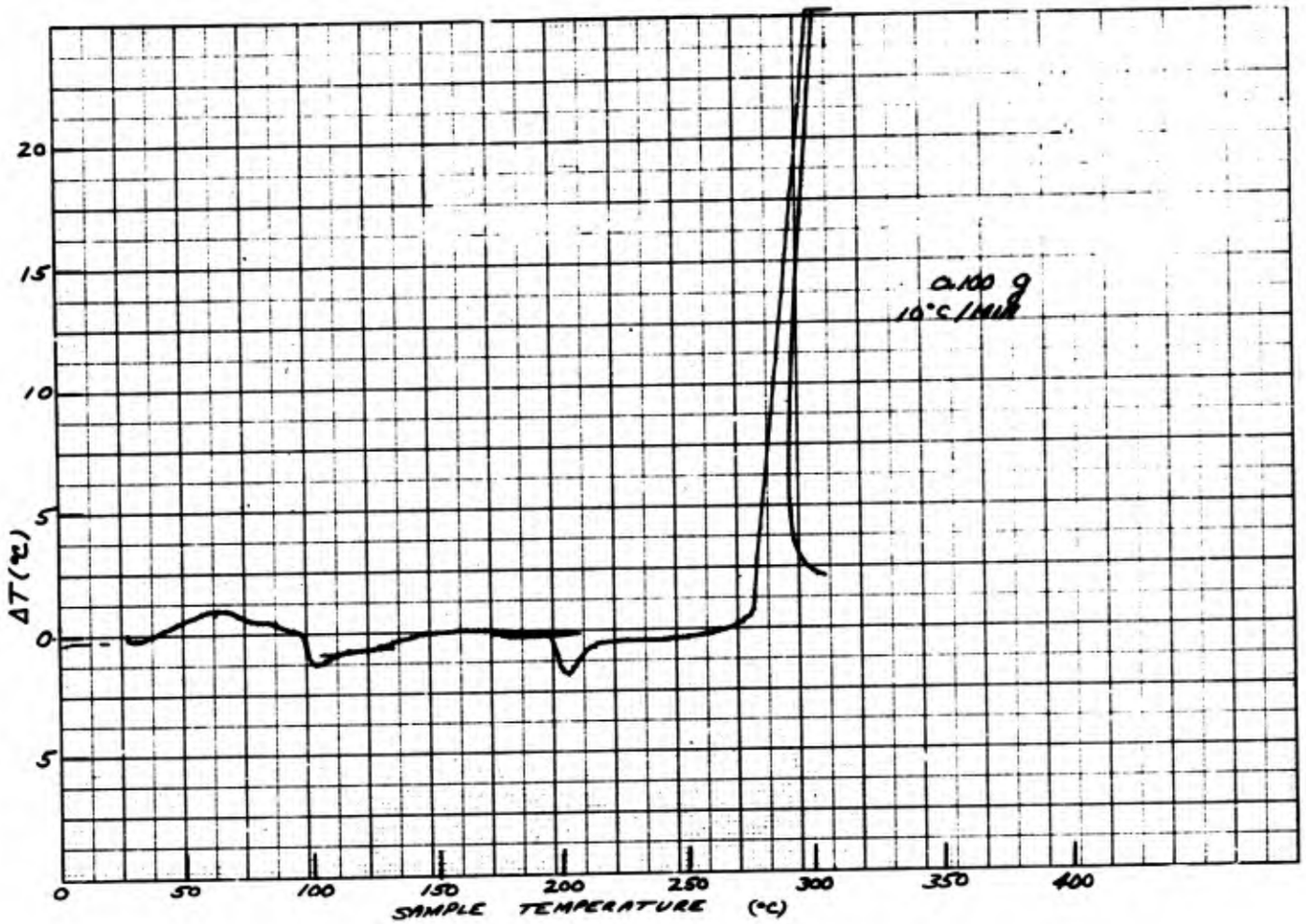

Fig 6a DTA curve for standard HMX/EXON (9505)

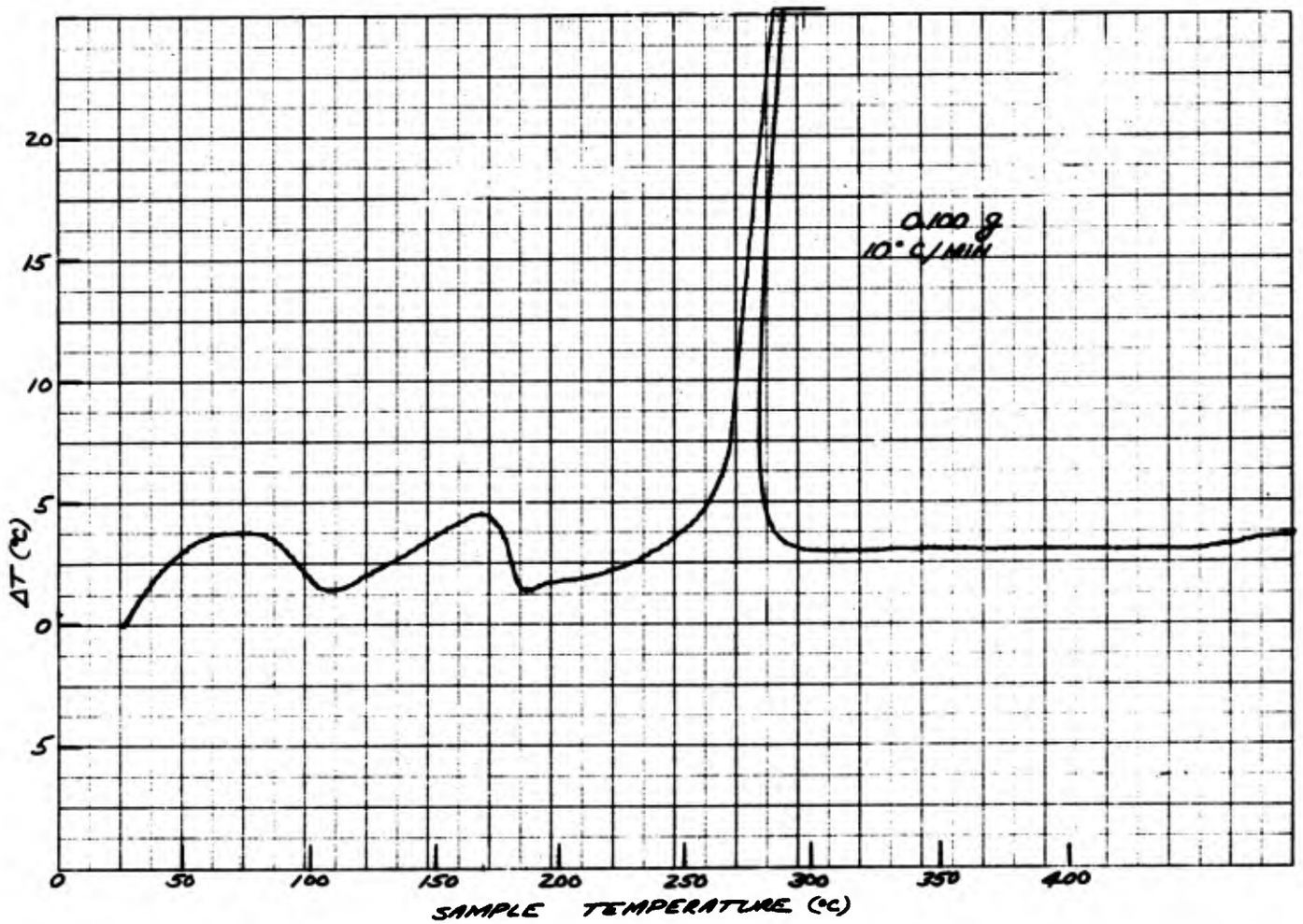

Fig 6b DTA curve for irradiated HMX/EXON (9505), Sample B12

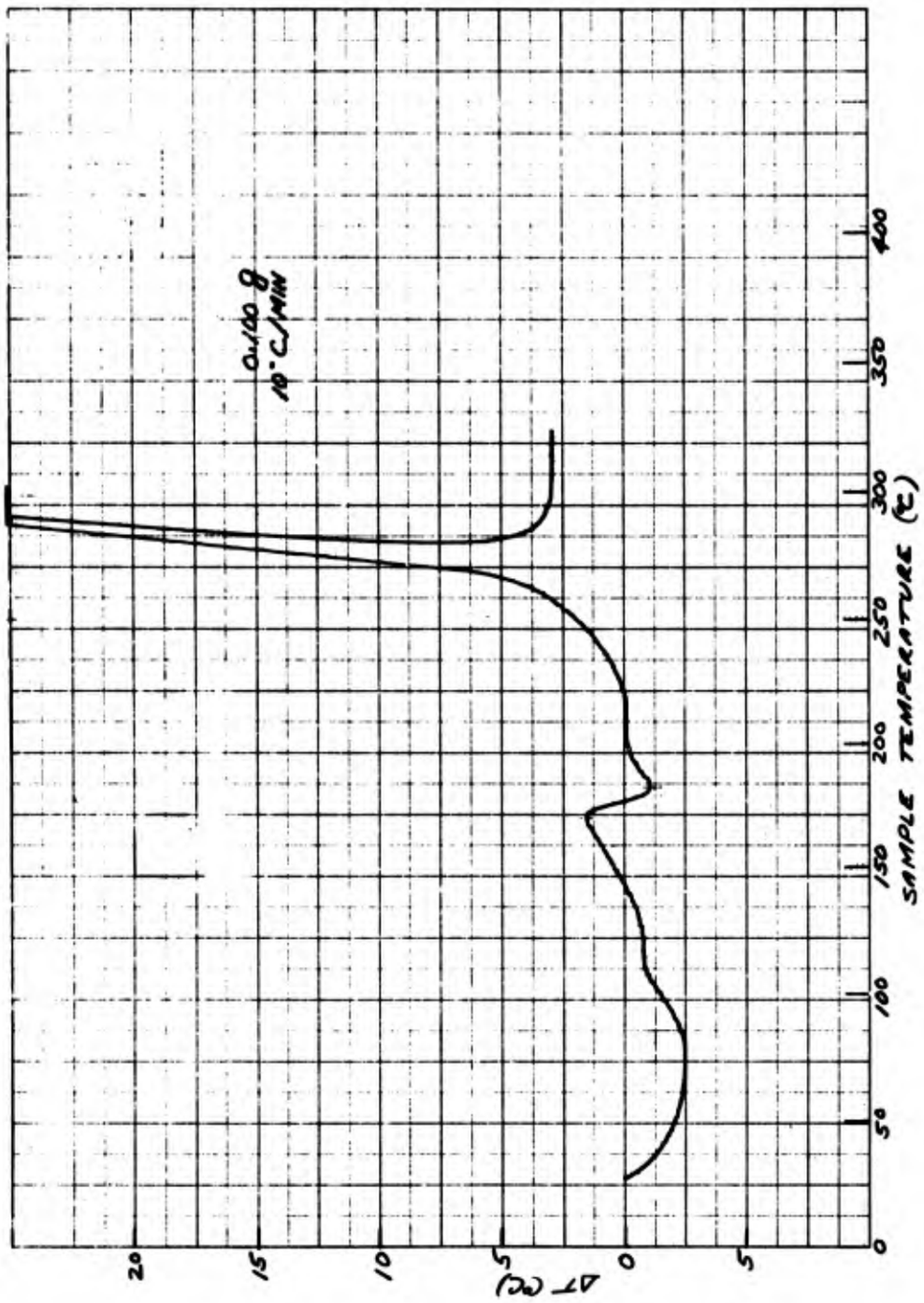

Fig 6c DTA curve for irradiated HMX/EXON (9505), Sample B13

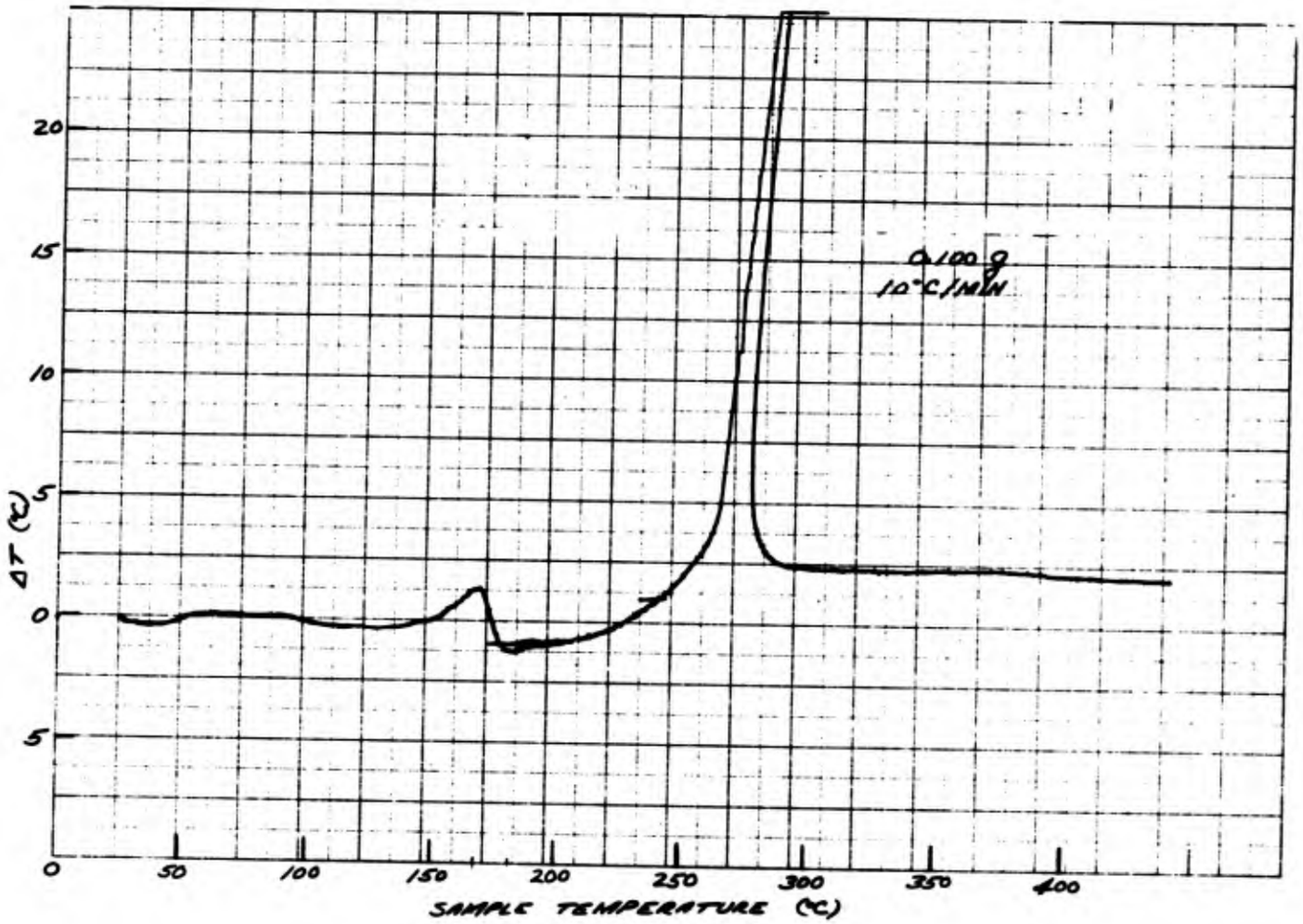

Fig 6d DTA curve for irradiated HMX/EXON (9505), Sample B14

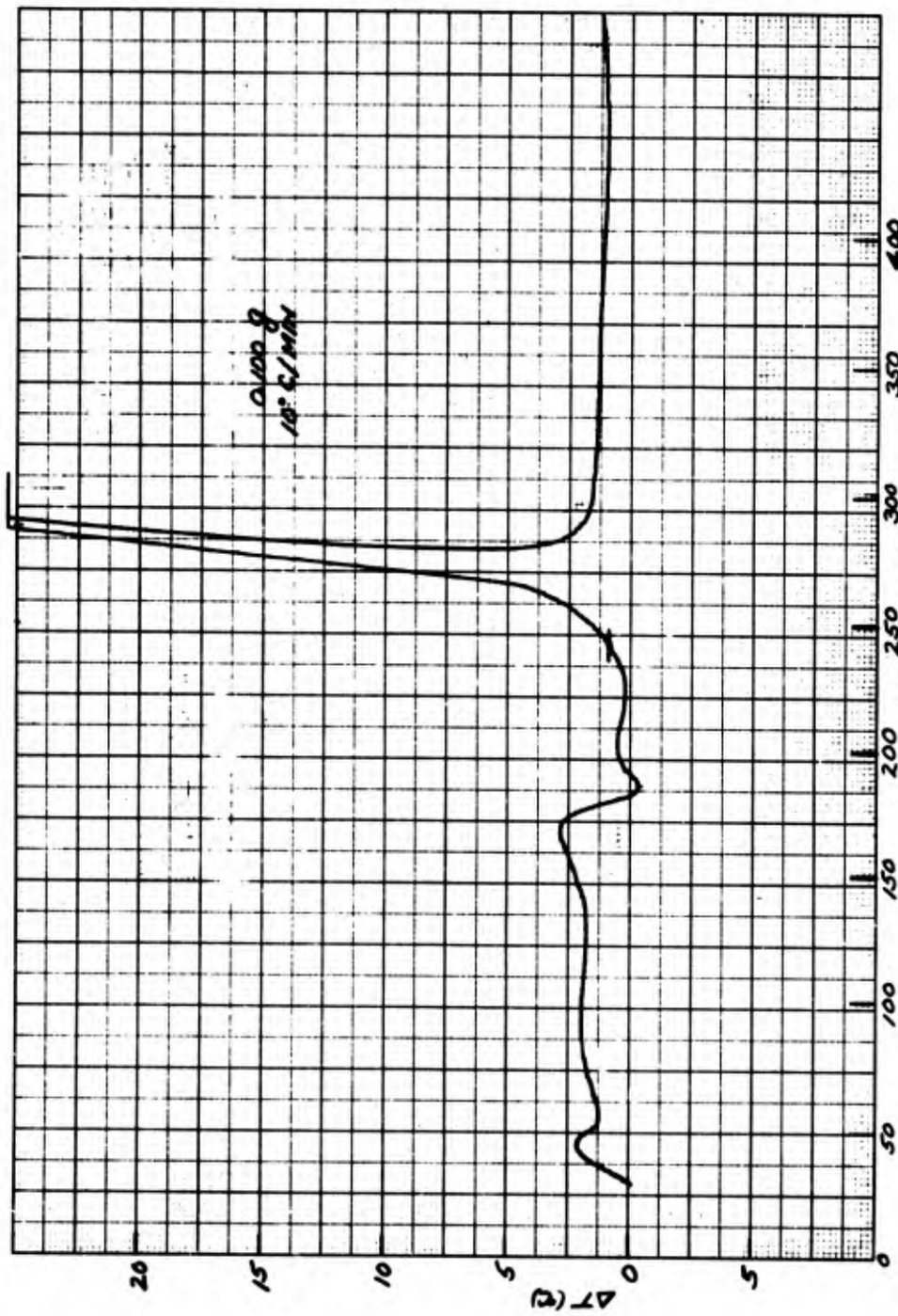

Fig 6e DTA curve for irradiated HMX/EXON (9505), Sample B25

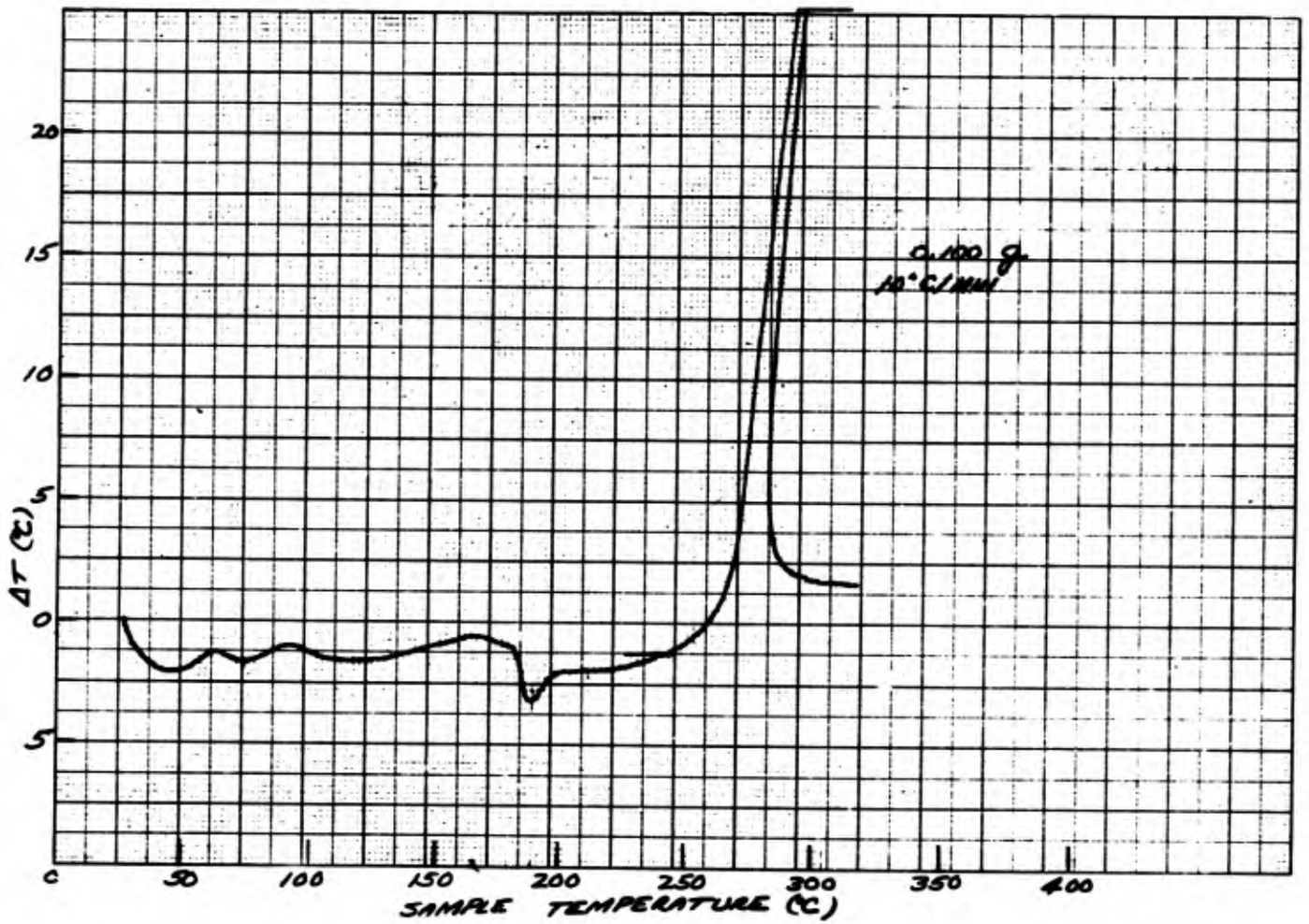

Fig 6f DTA curve for irradiated HMX/EXON (9505), Sample B21

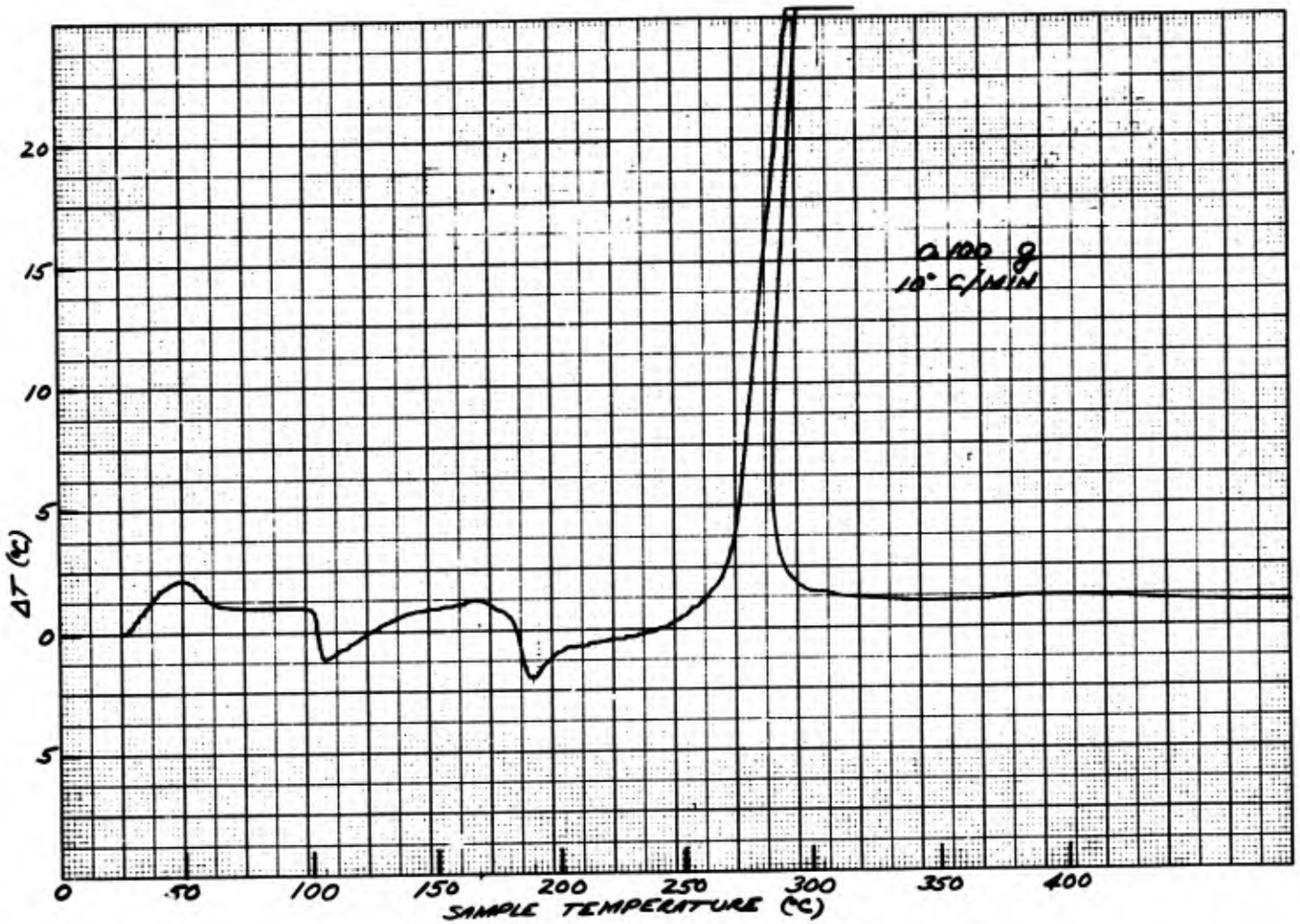

Fig 6g DTA curve for irradiated HMX/EXON (9505), Sample B22

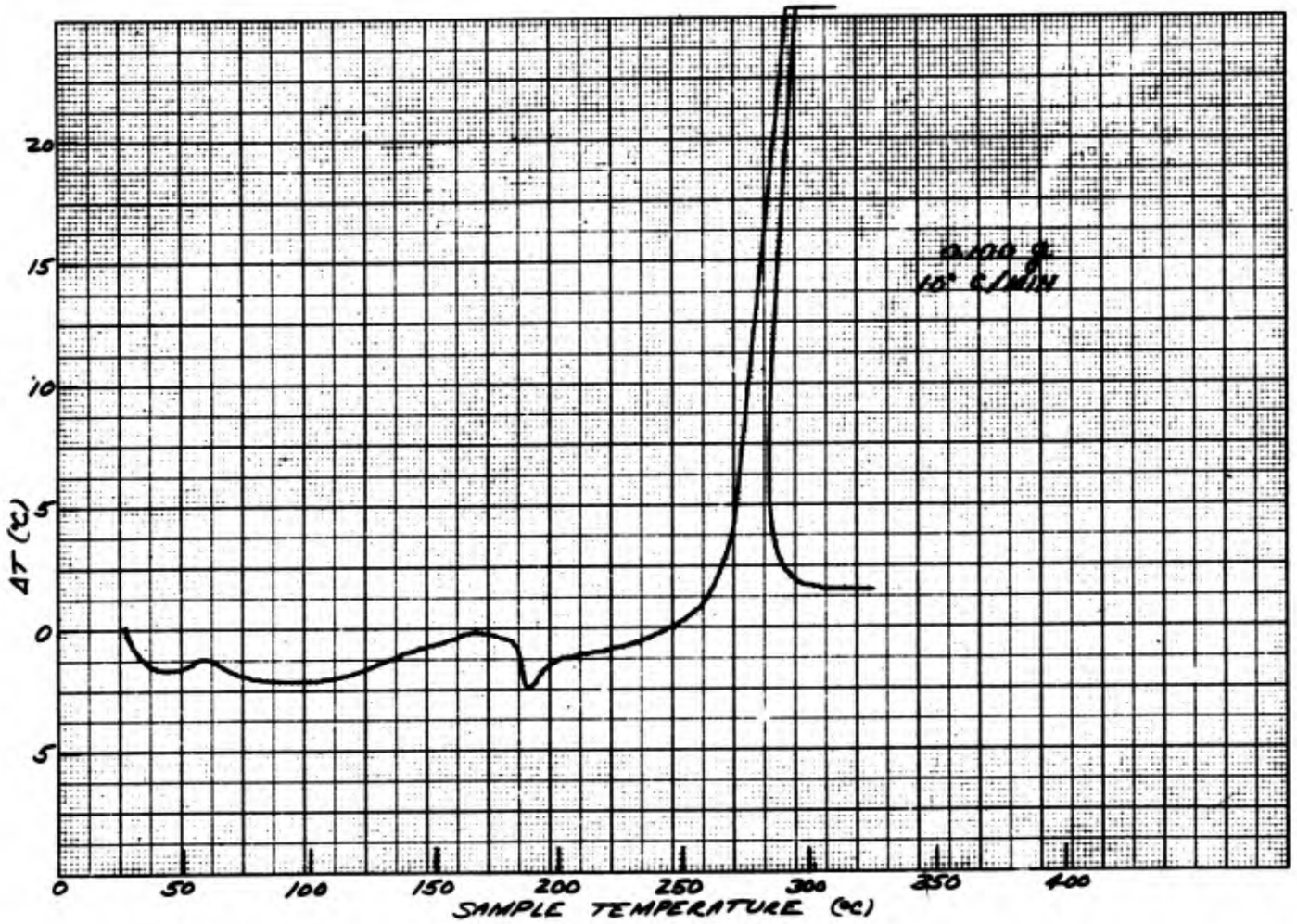

Fig 6h DTA curve for irradiated HMX/EXON (9505), Sample B24

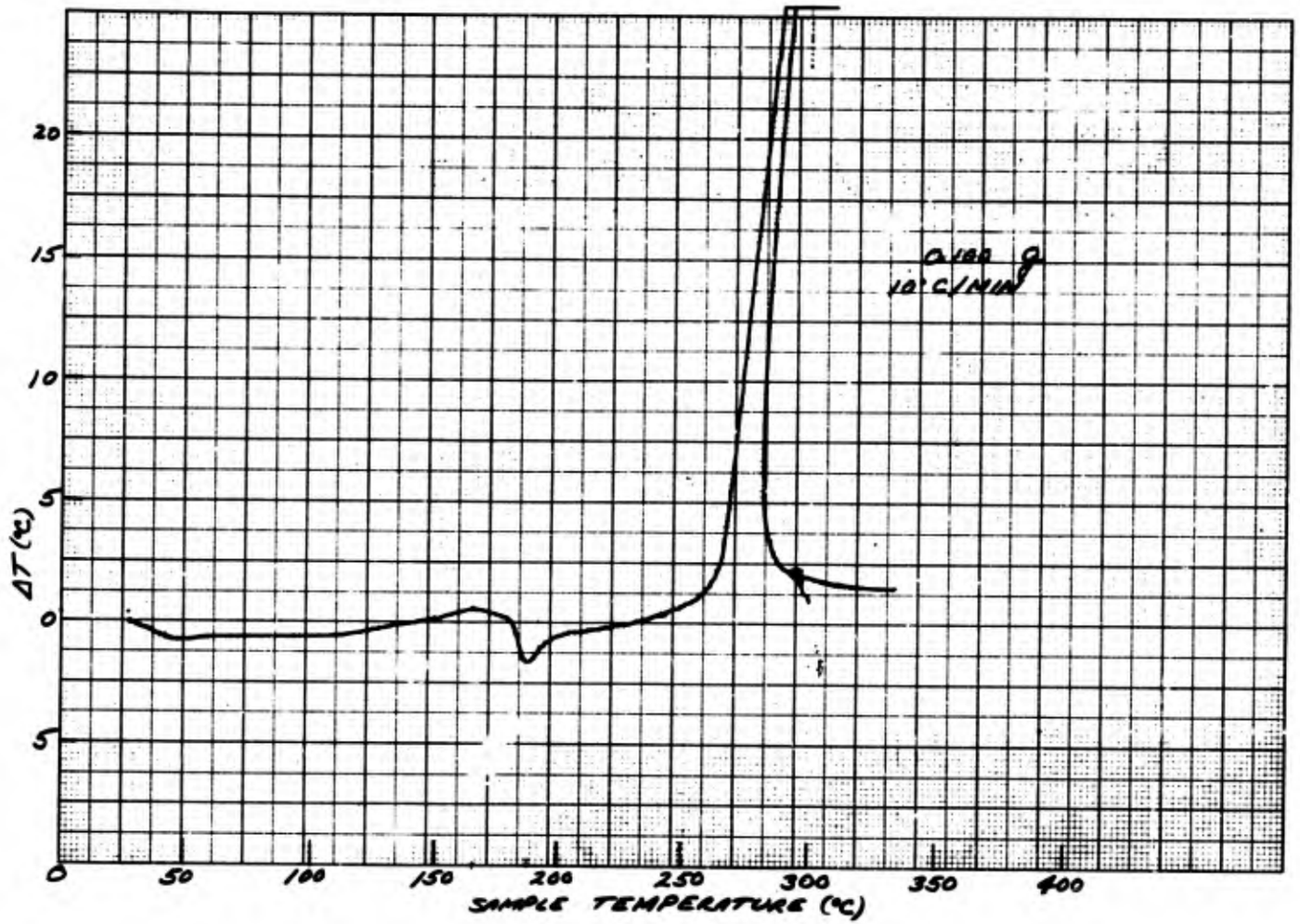

Fig 6i DTA curve for irradiated HMX/EXON (9505), Sample B26

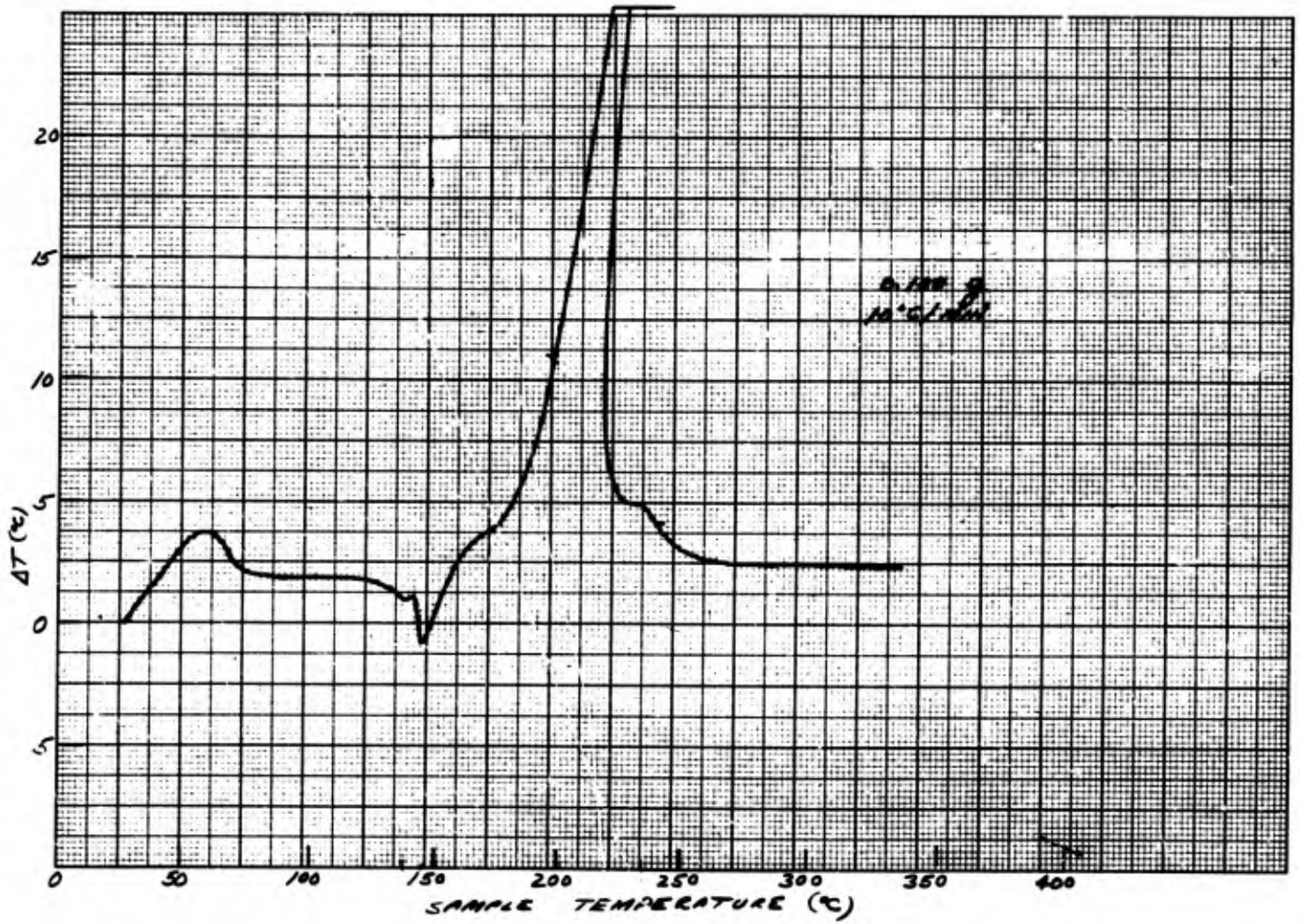

Fig 7a DTA curve for standard PETN

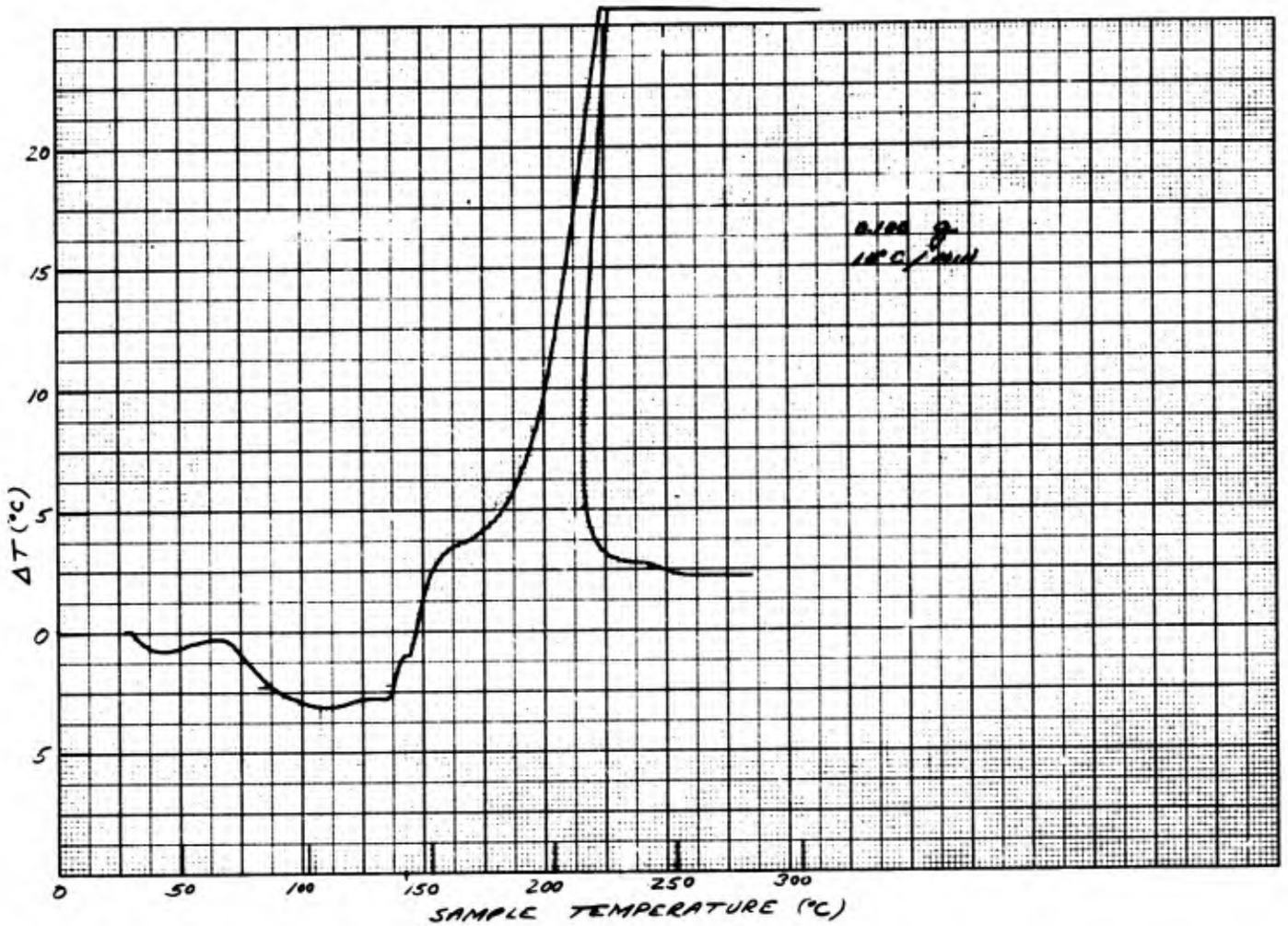

Fig 7b DTA curve for irradiated PETN, Sample D12

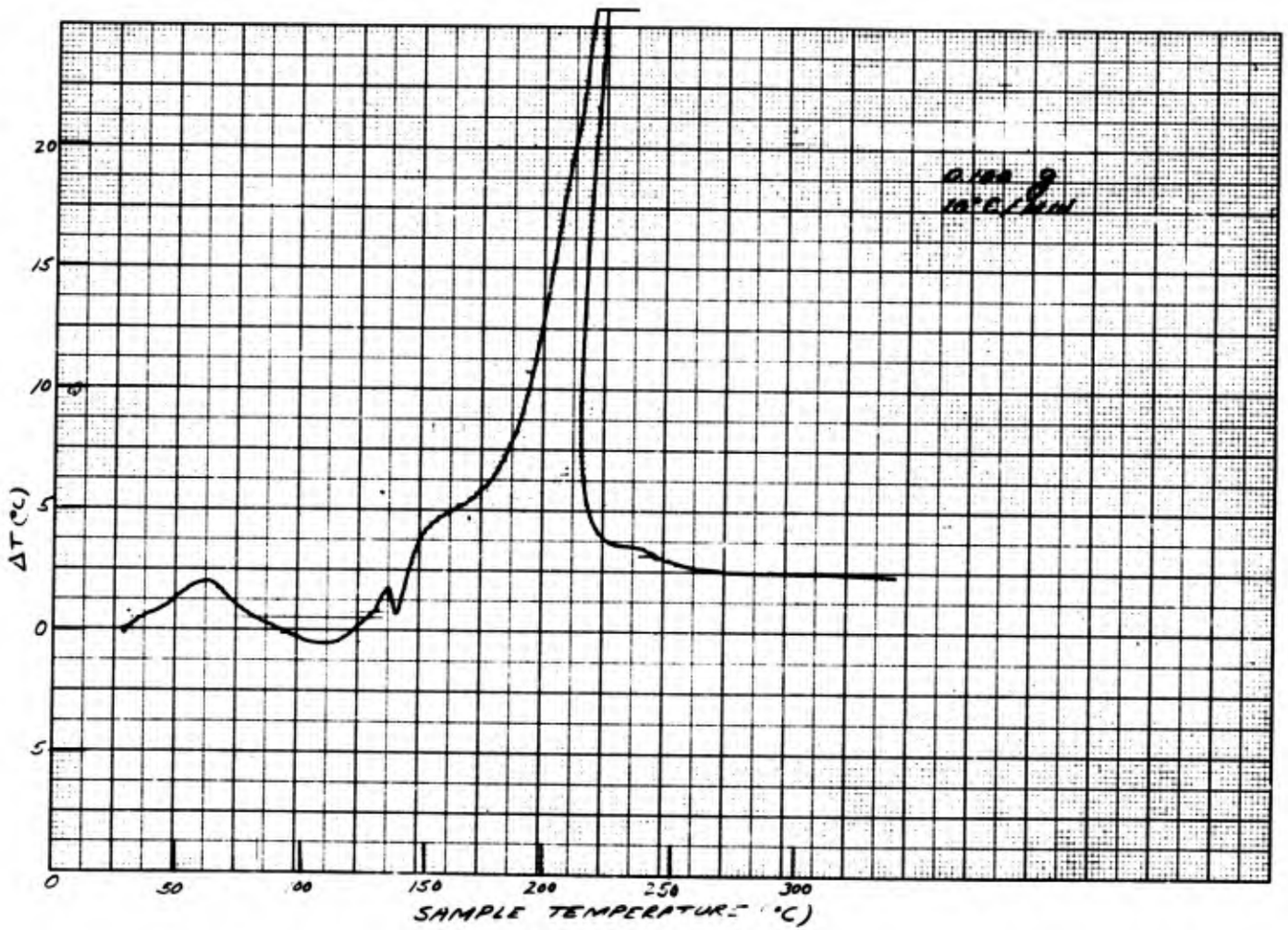

Fig 7c DTA curve for irradiated PETN, Sample D13

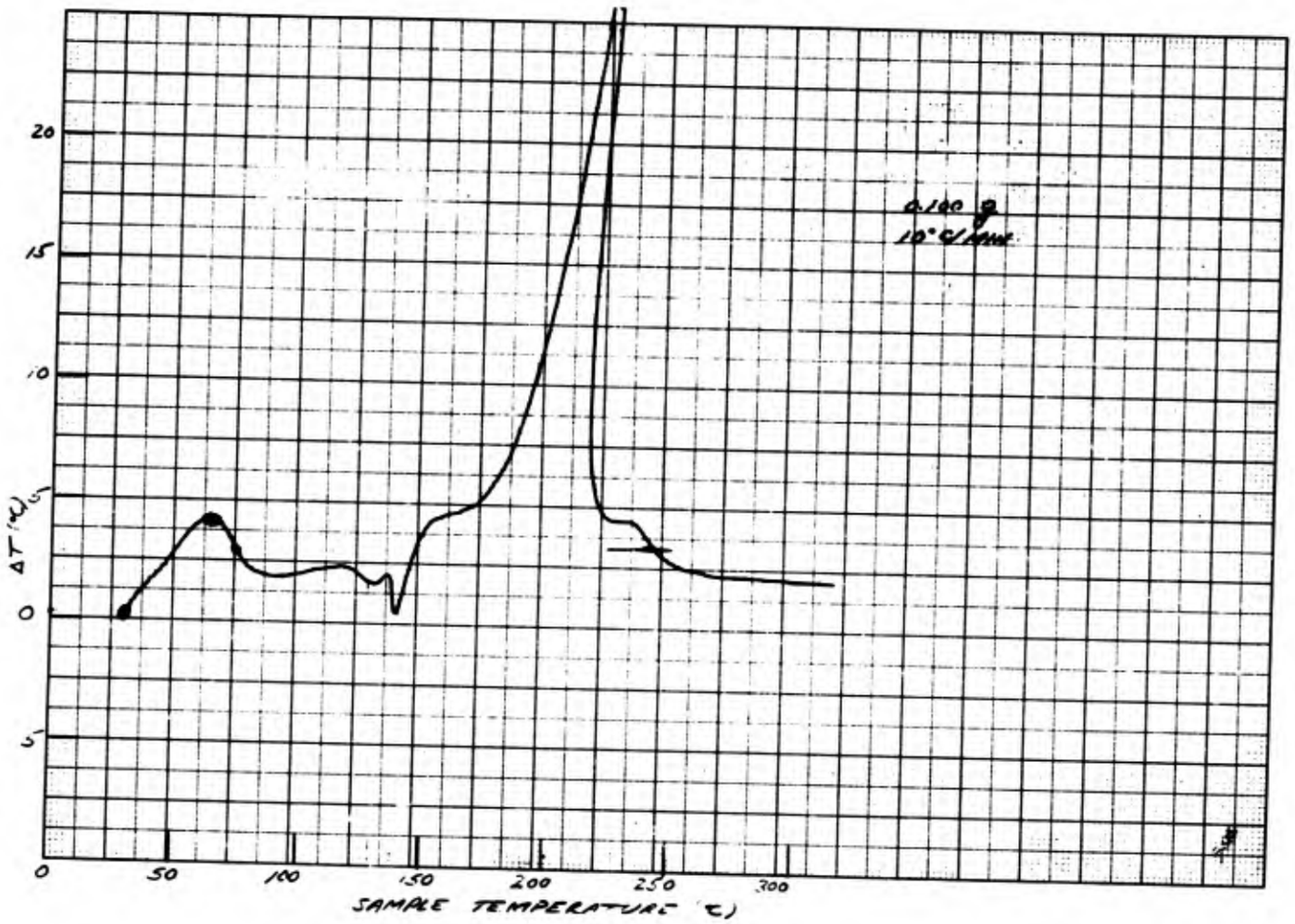

Fig 7d DTA curve for irradiated PETN, Sample D21

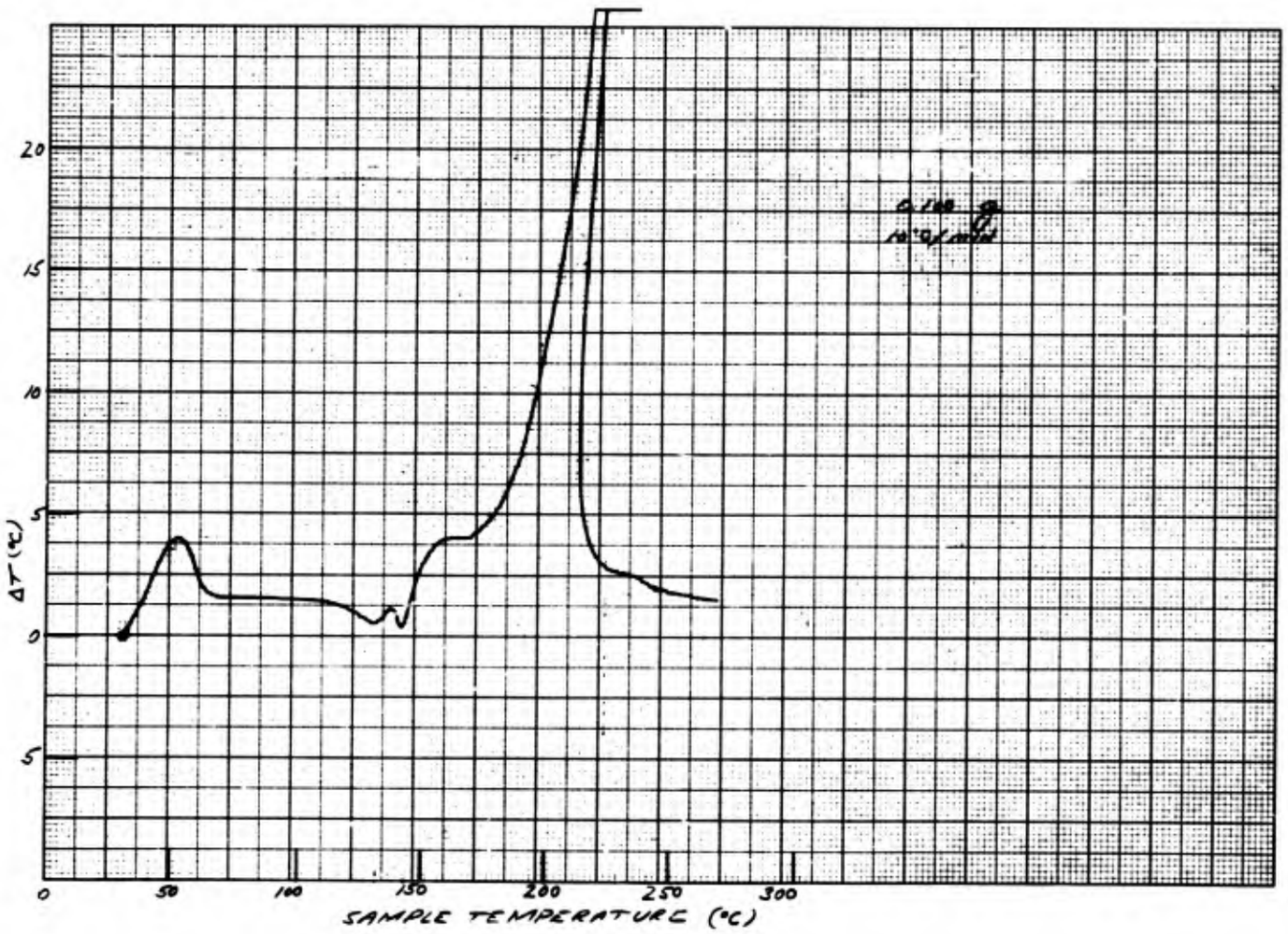

Fig 7e DTA curve for irradiated PETN, Sample D14

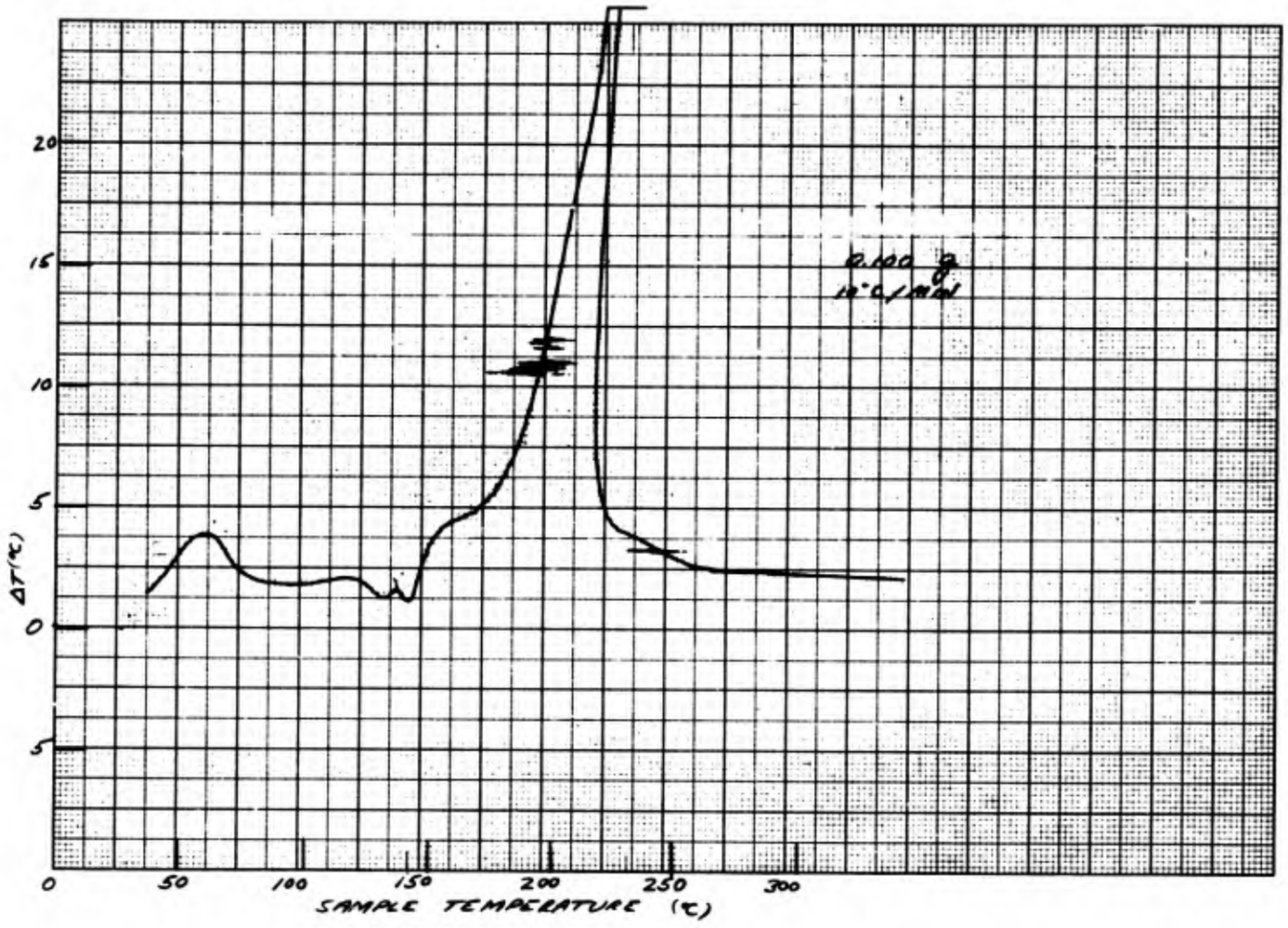

Fig 7f DTA curve for irradiated PETN, Sample D22

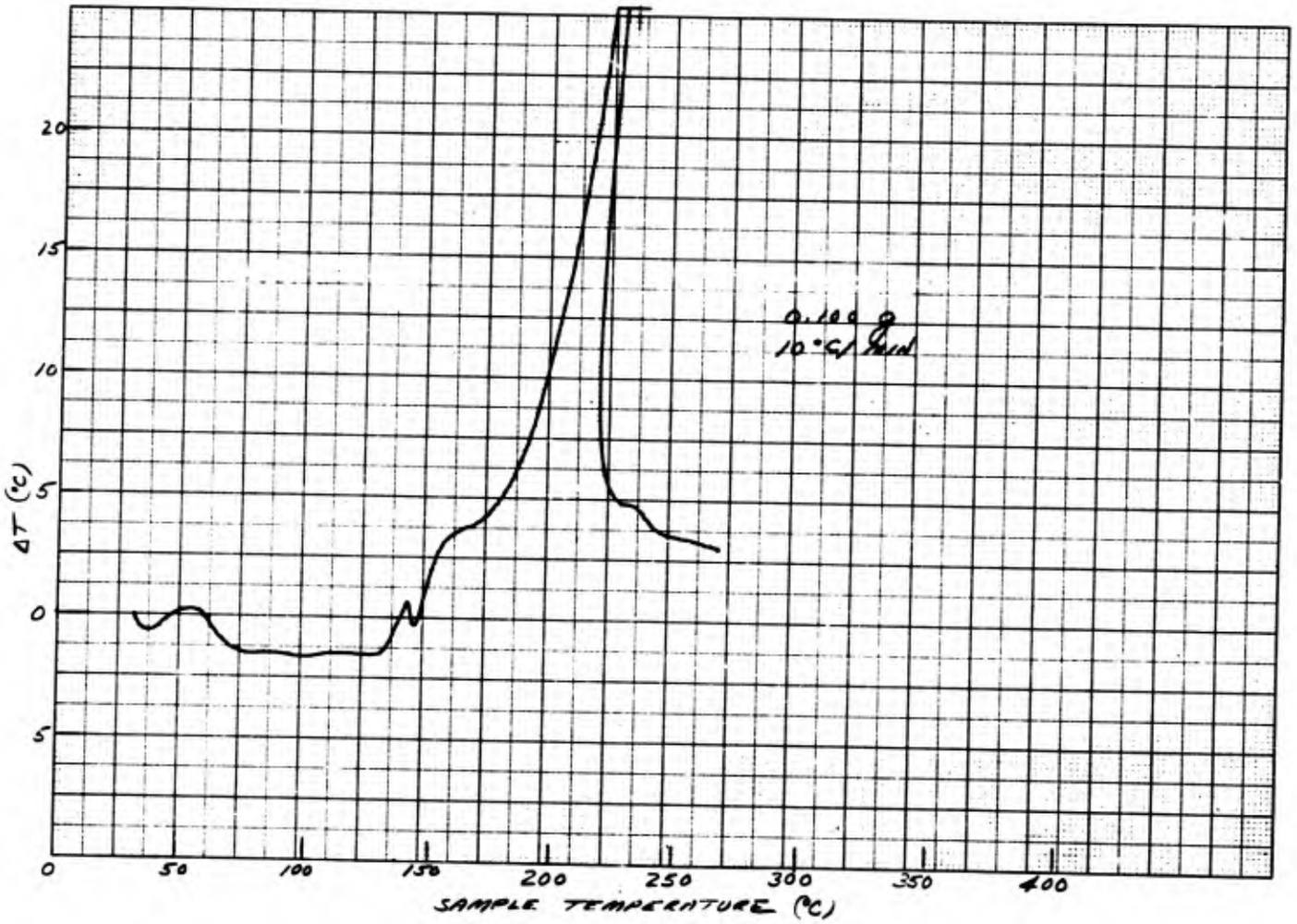

Fig 7g DTA curve for irradiated PETN, Sample D24

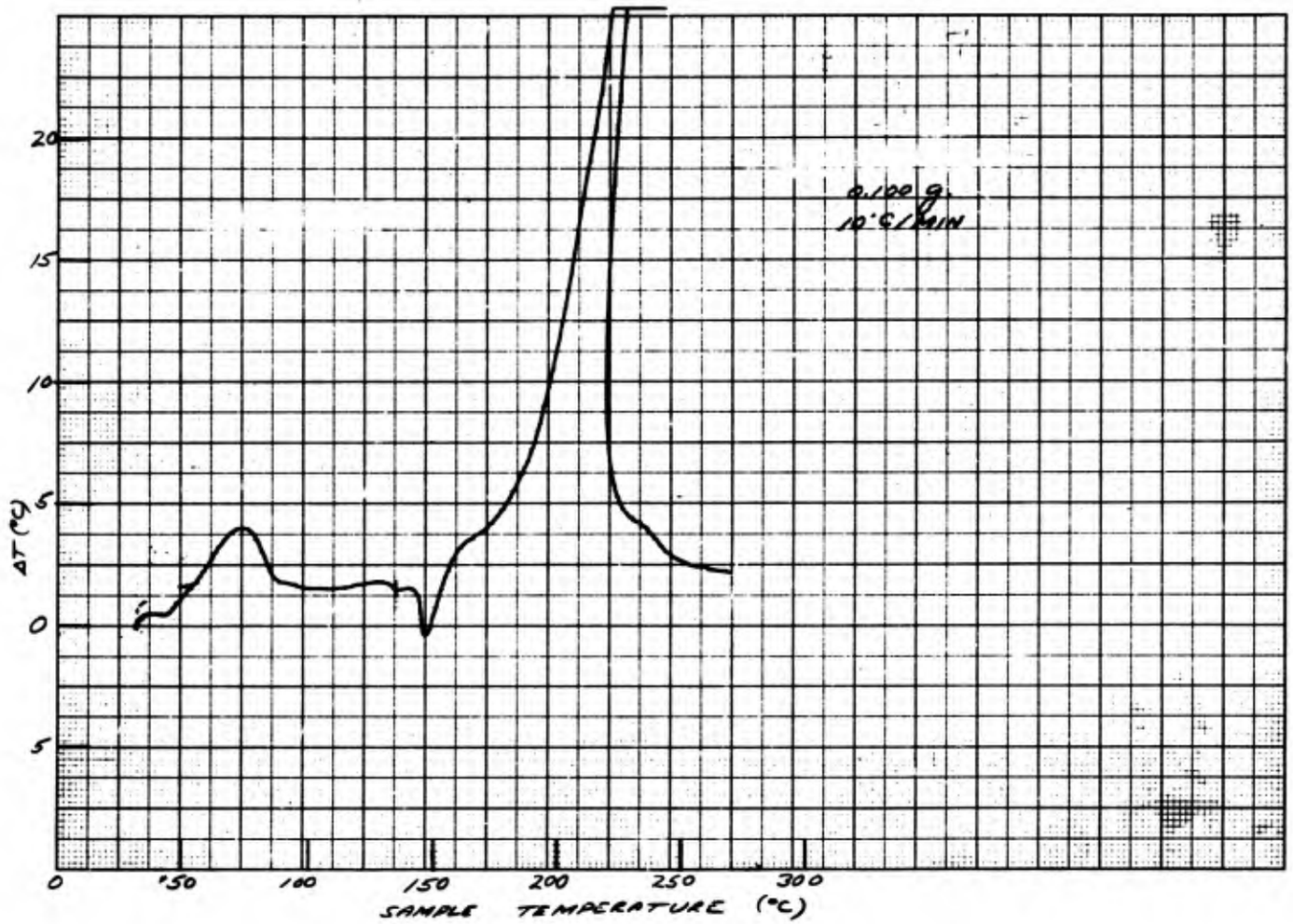

Fig 7h DTA curve for irradiated PETN, Sample D25

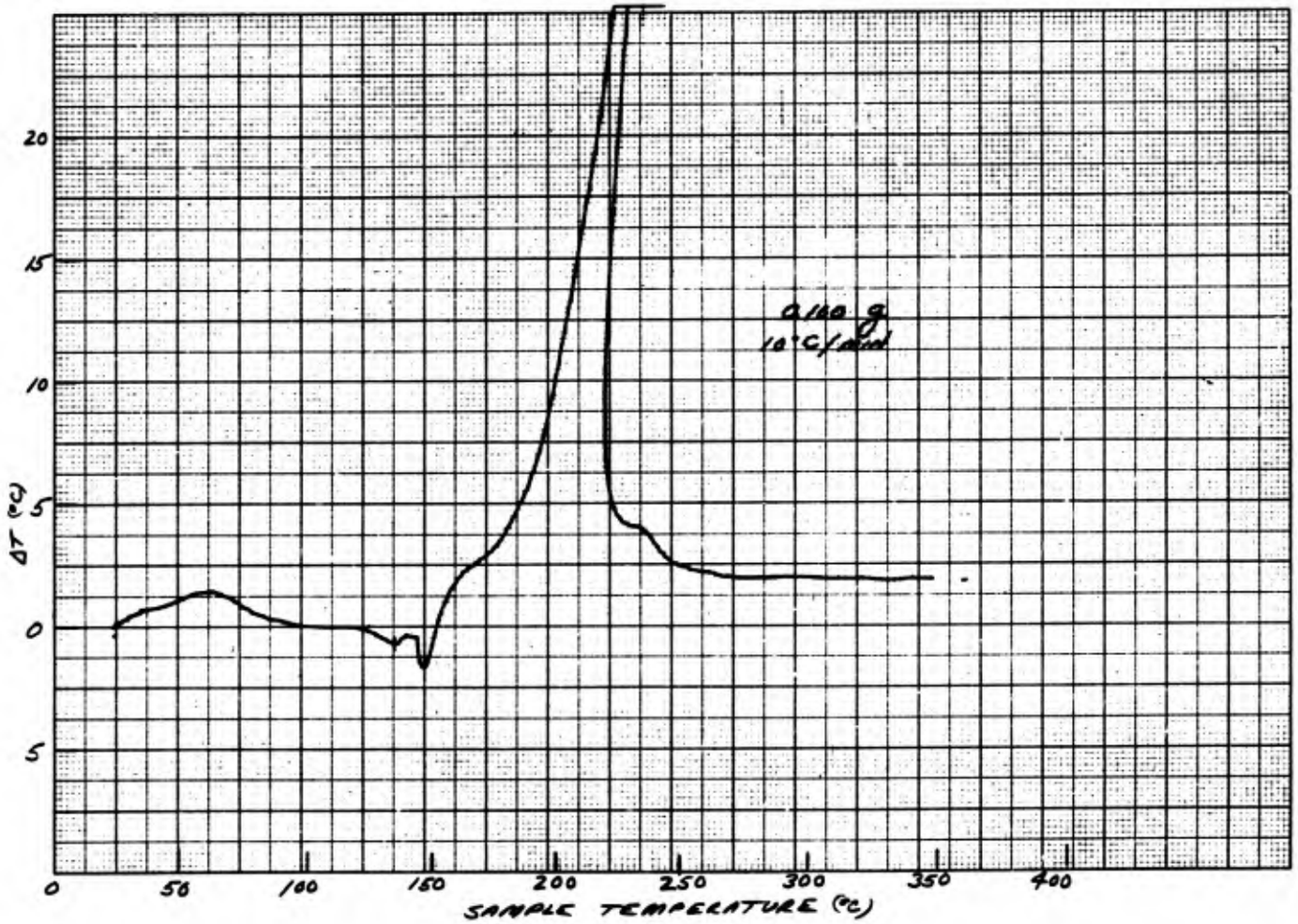

Fig 7i DTA curve for irradiated PETN, Sample D26

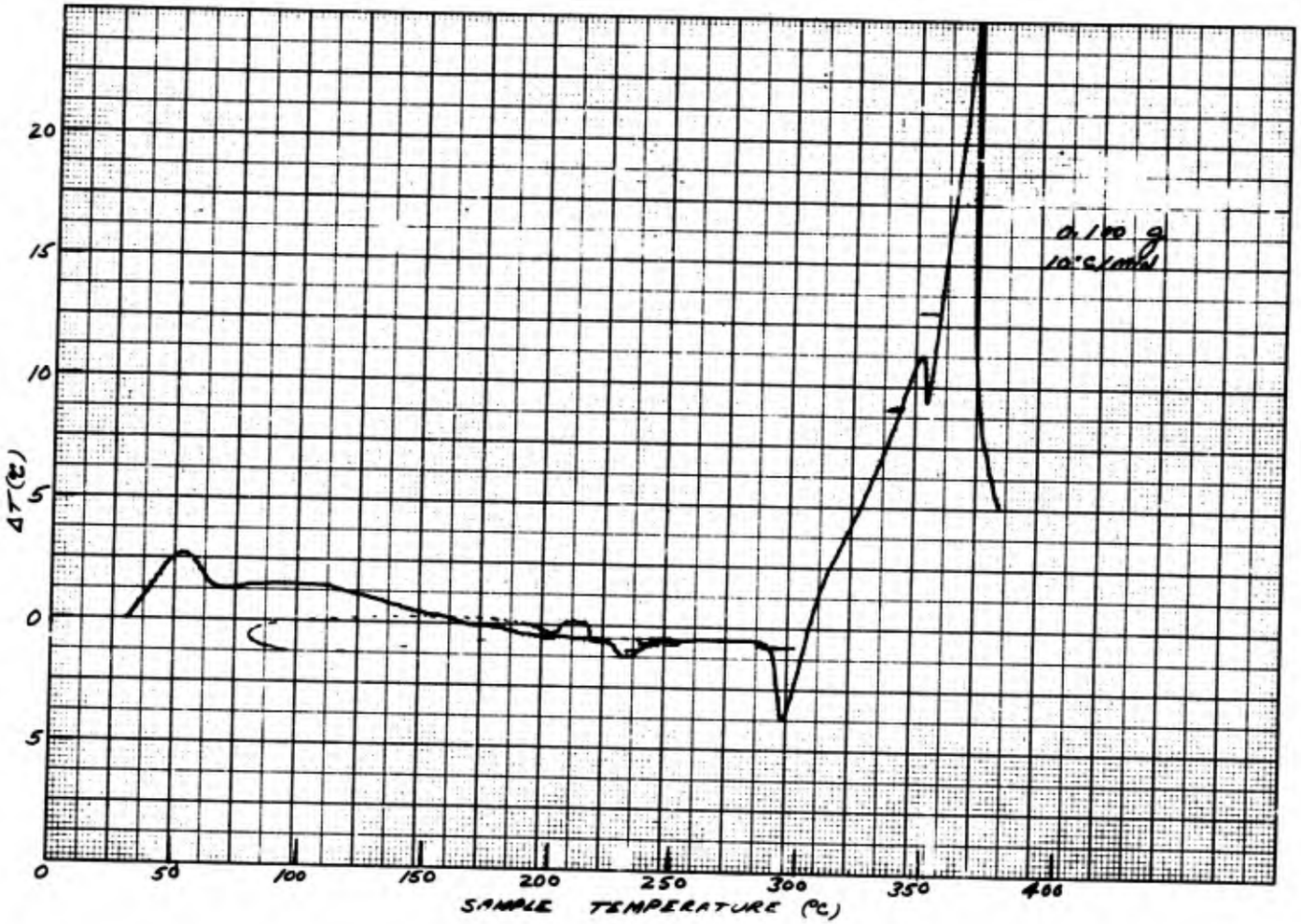

Fig 8a DTA curve for standard DATB

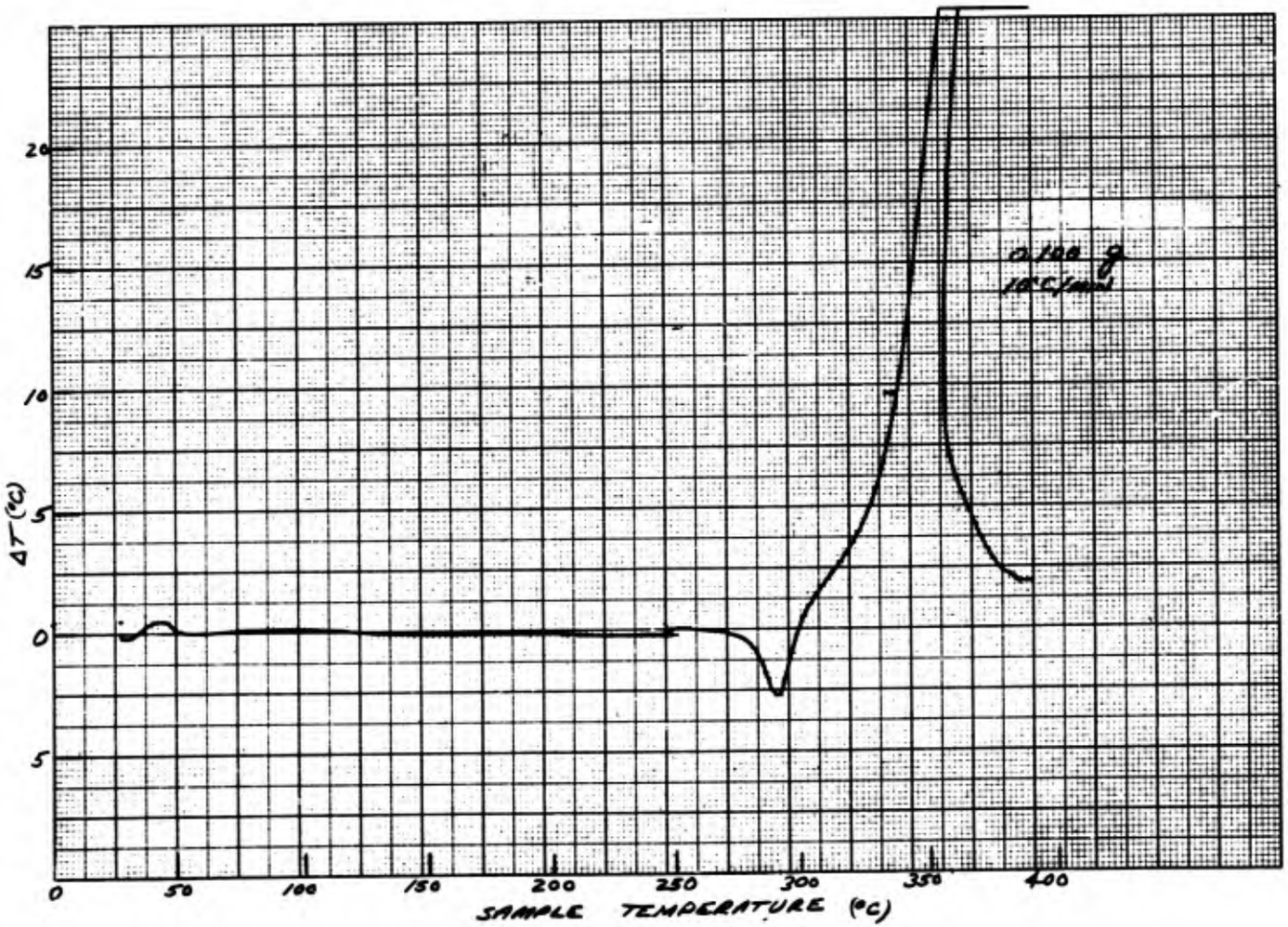

Fig 8b DTA curve for irradiated DATB, Sample C21

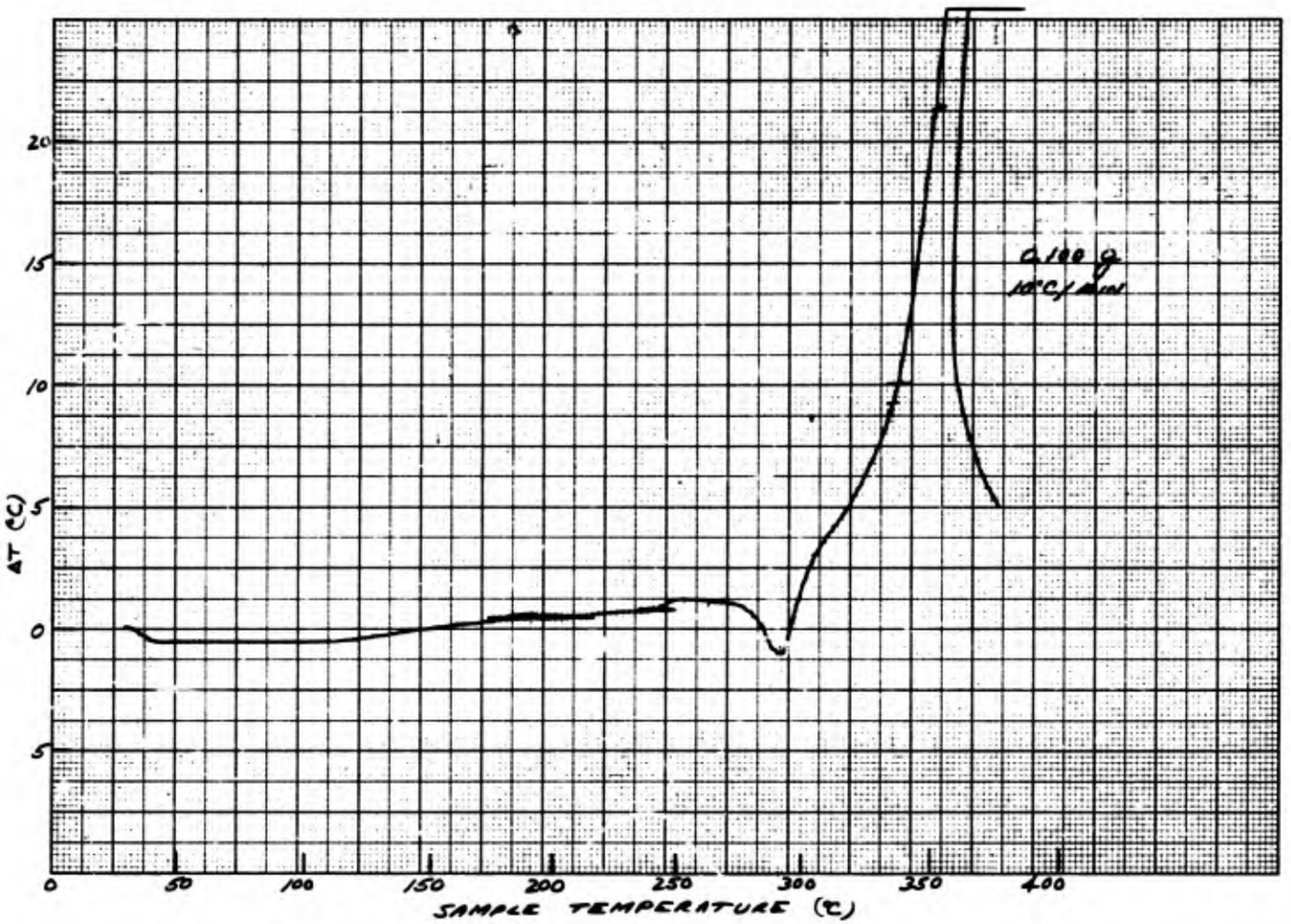

Fig 8c DTA curve for irradiated DATB, Sample C22

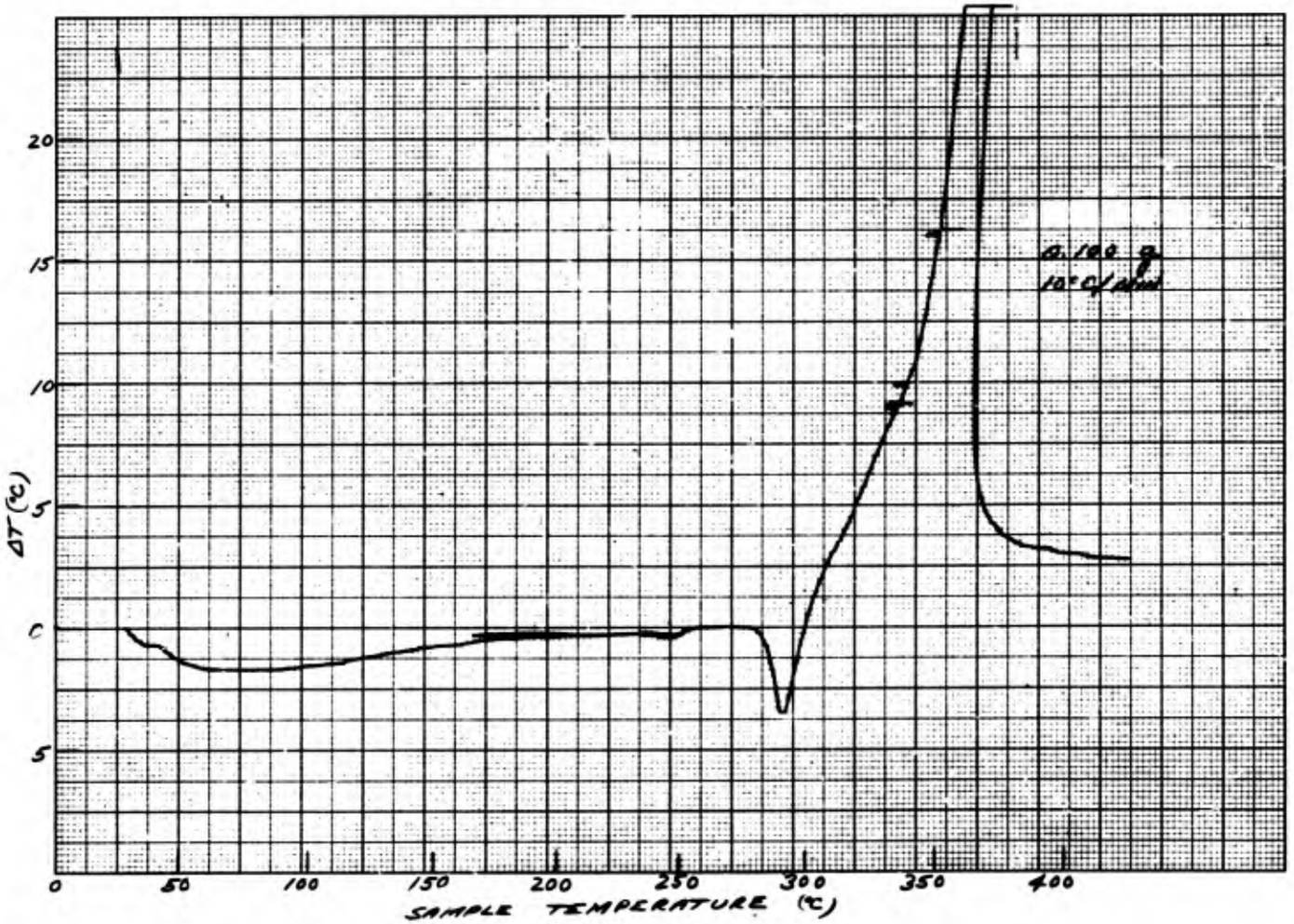

Fig 8d DTA curve for irradiated DATB, Sample C23

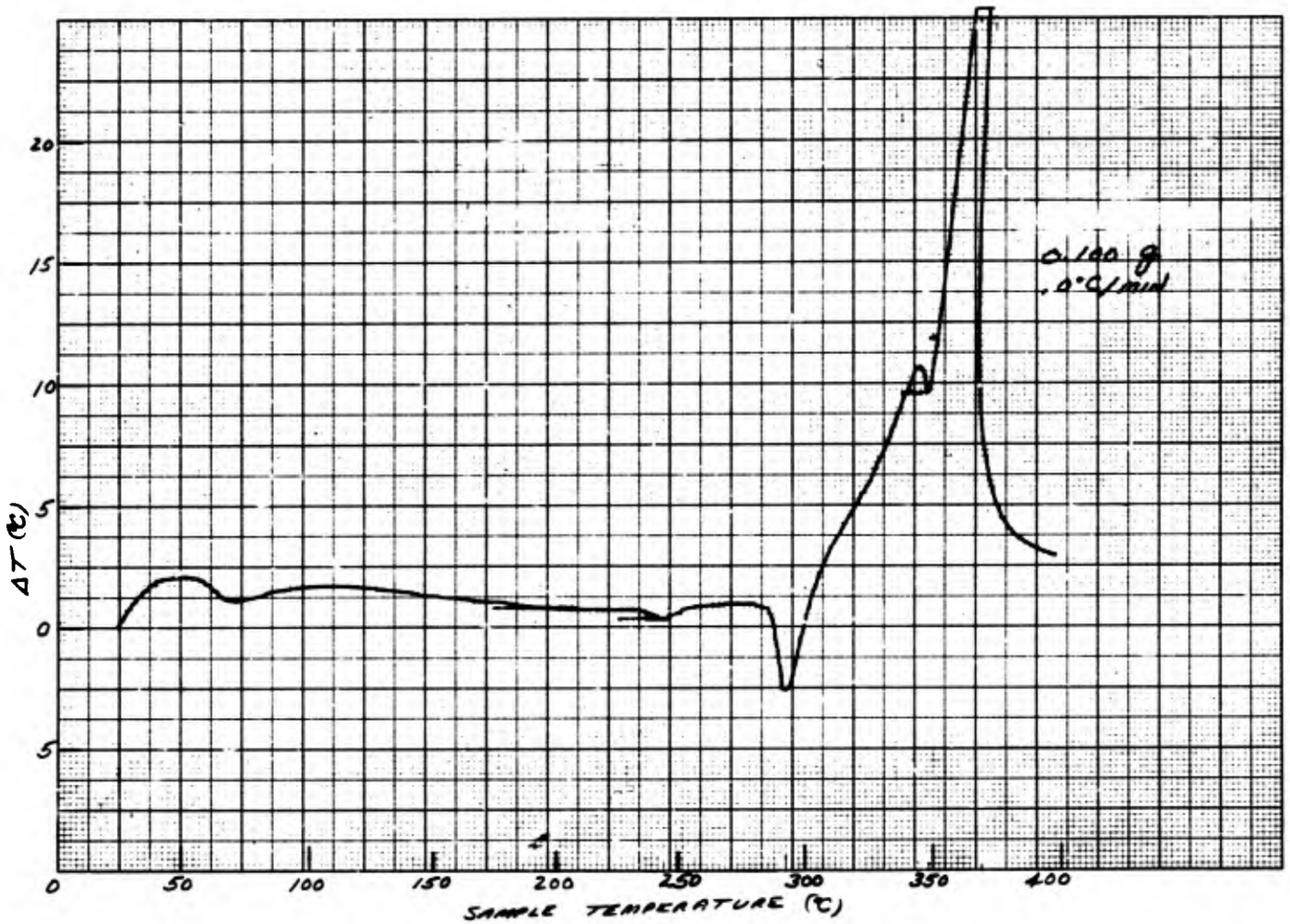

Fig 8e DTA curve for irradiated DATB, Sample C14

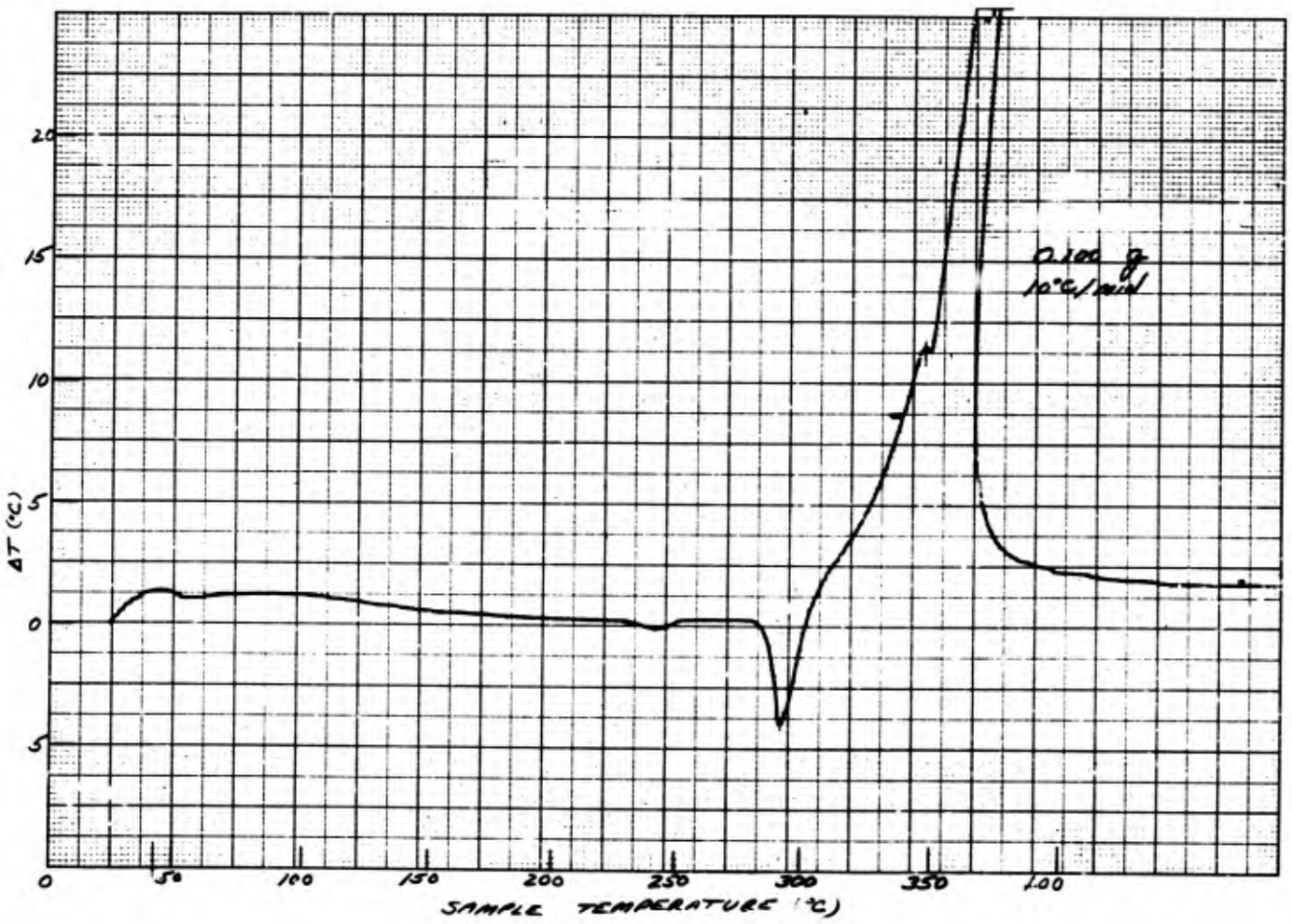

Fig 8f DTA curve for irradiated DATB, Sample C13

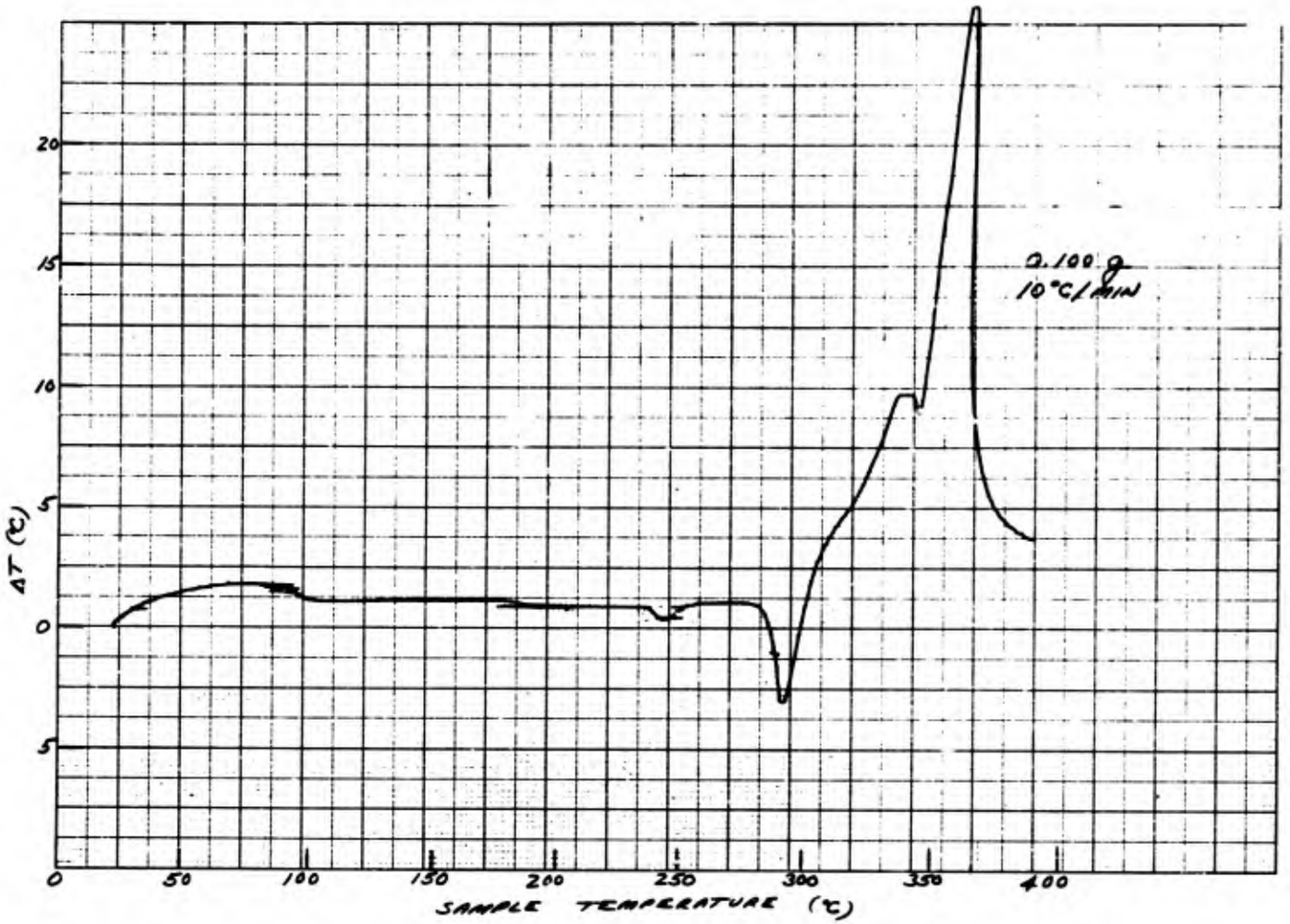

Fig 8g DTA curve for irradiated DATB, Sample C15

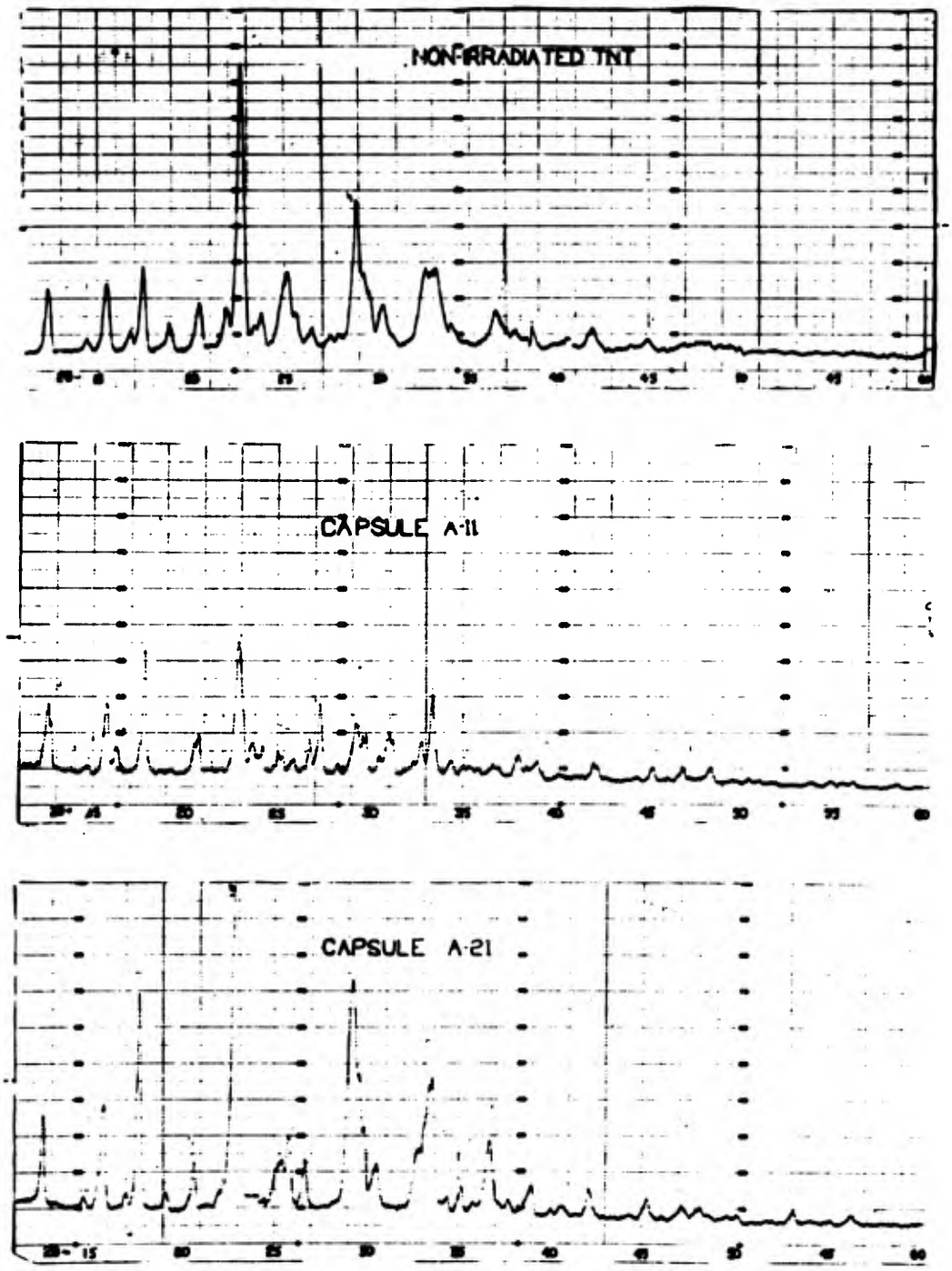

Fig 9 X-ray diffractograms for irradiated and standard TNT

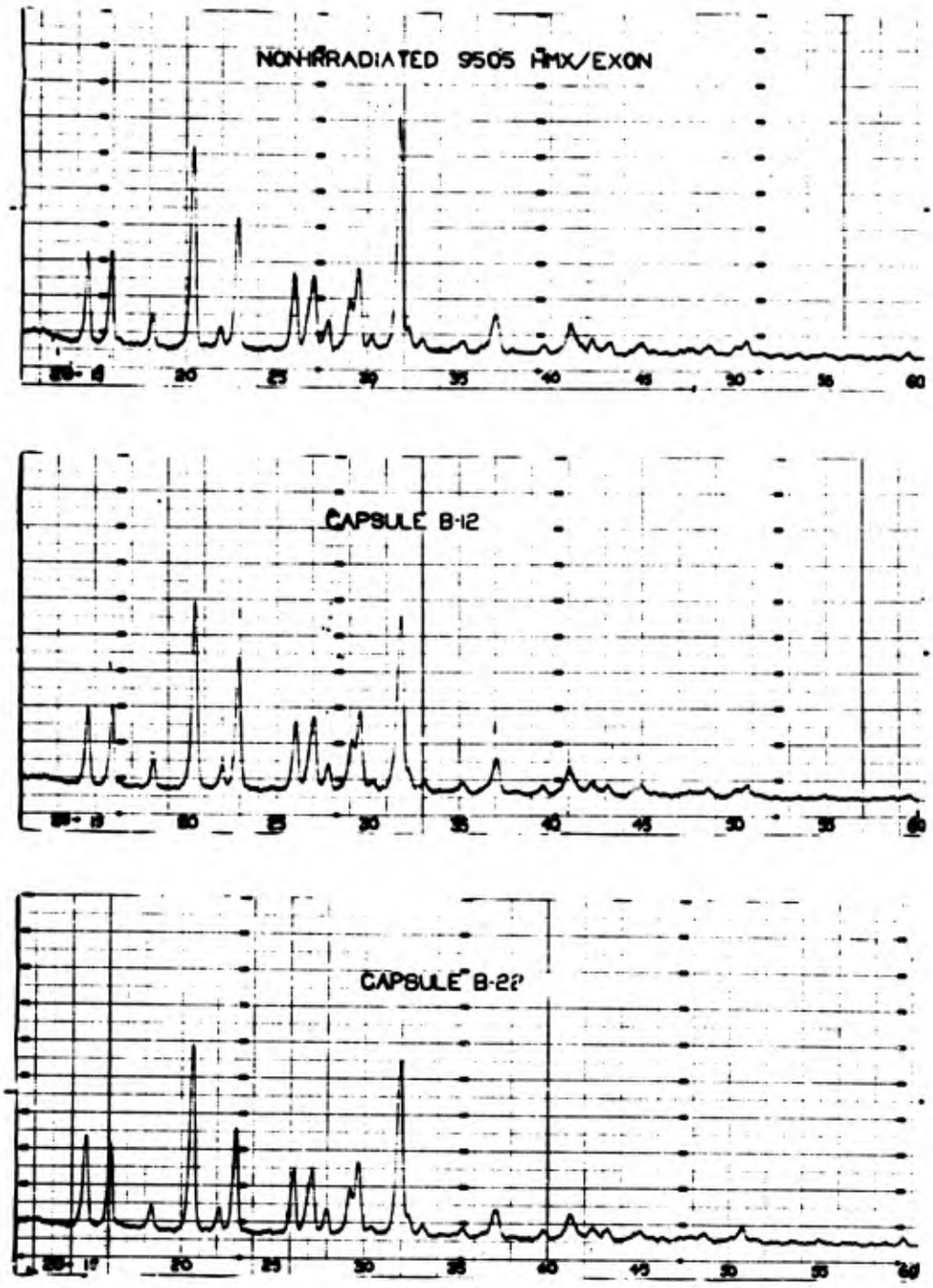

Fig 10 X-ray diffractograms for irradiated and standard HMX/EXON (9505)

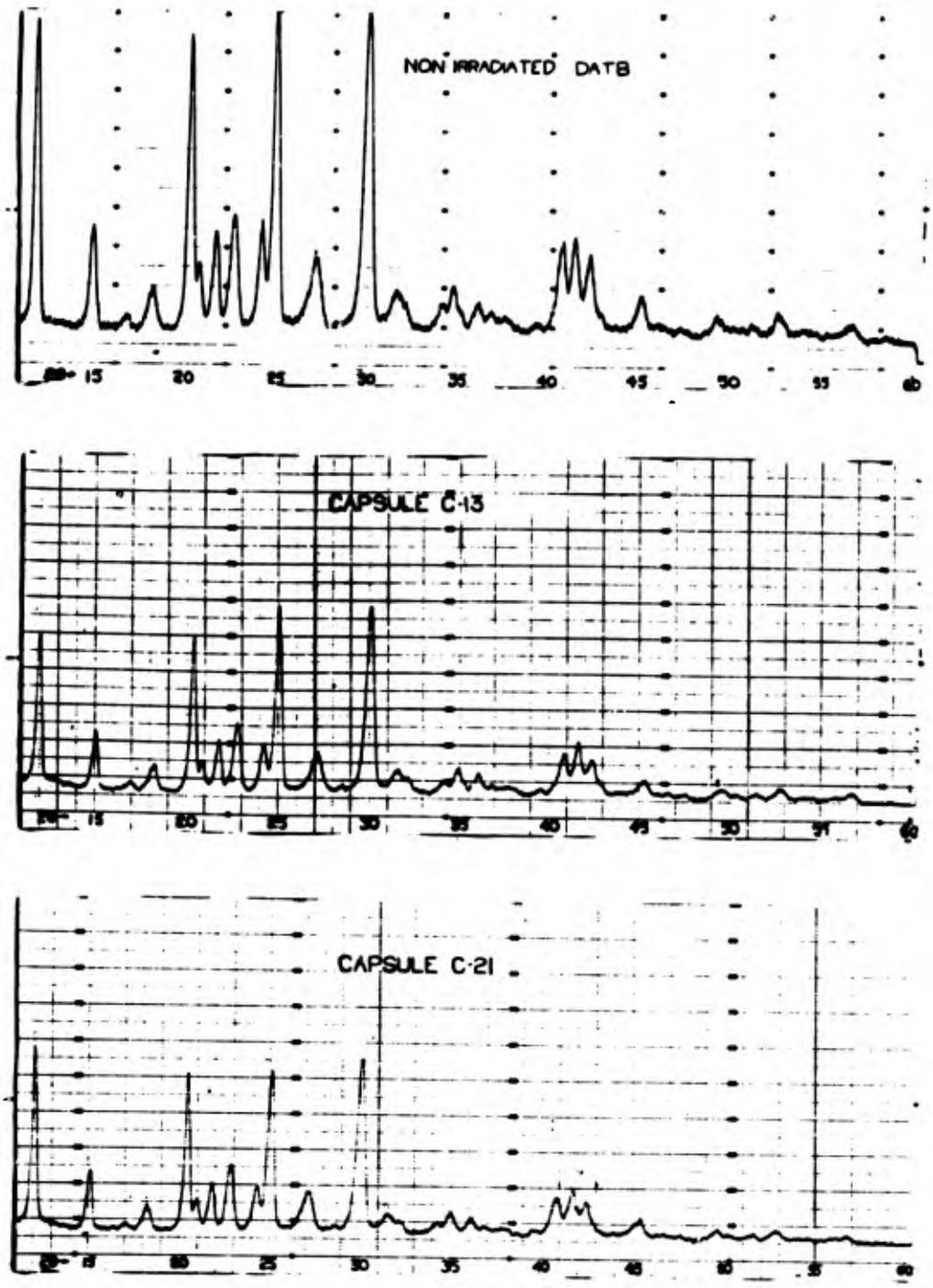

Fig 11 X-ray diffractograms for irradiated and standard DATB

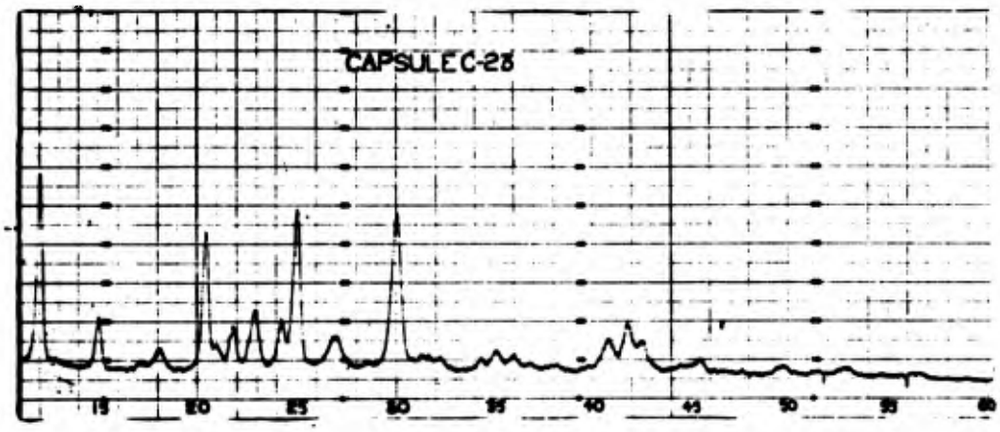

Fig 11 (cont) X-ray diffractograms for irradiated and standard DATB

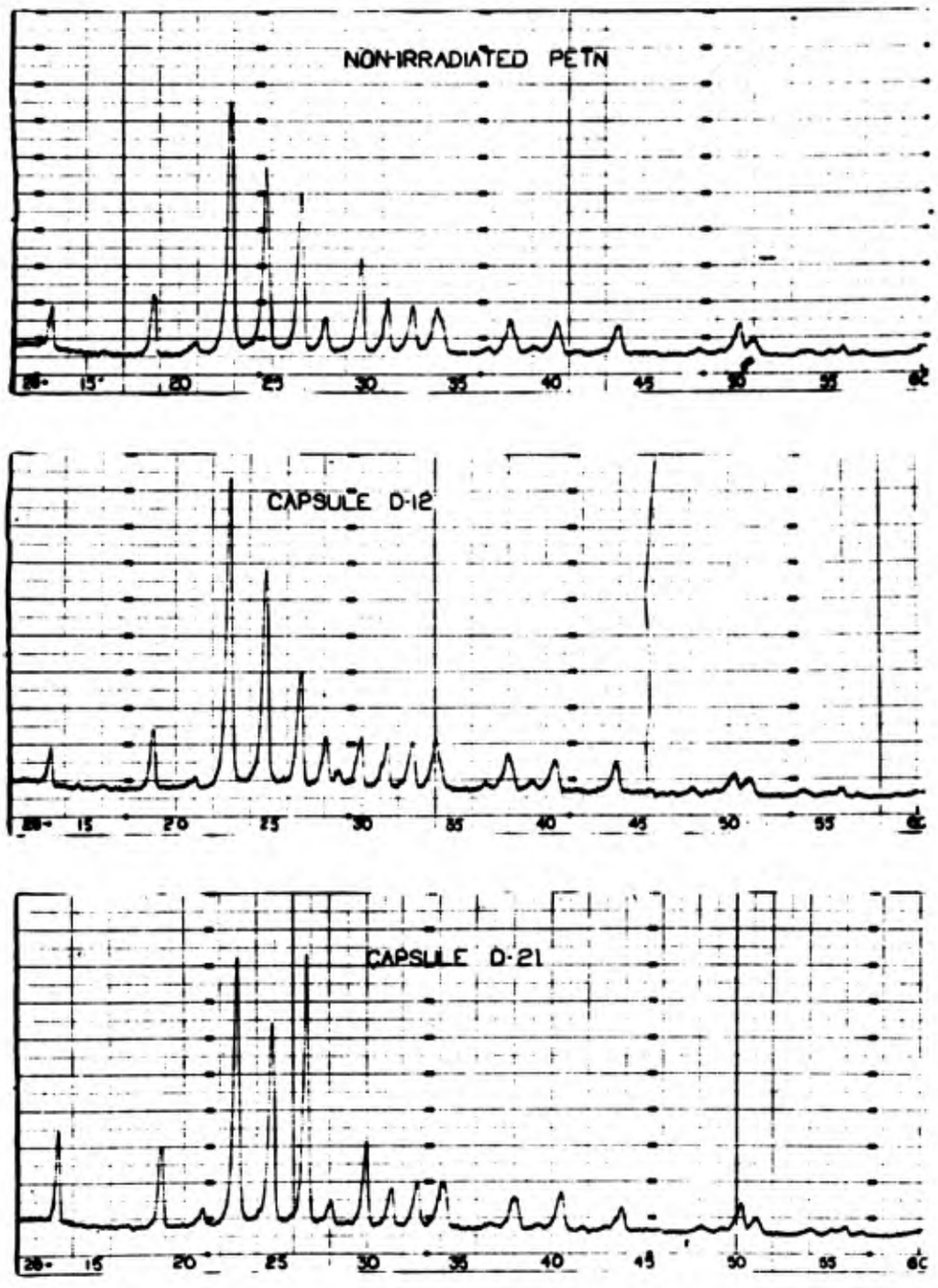

Fig 12 X-ray diffractograms for irradiated and standard PETN

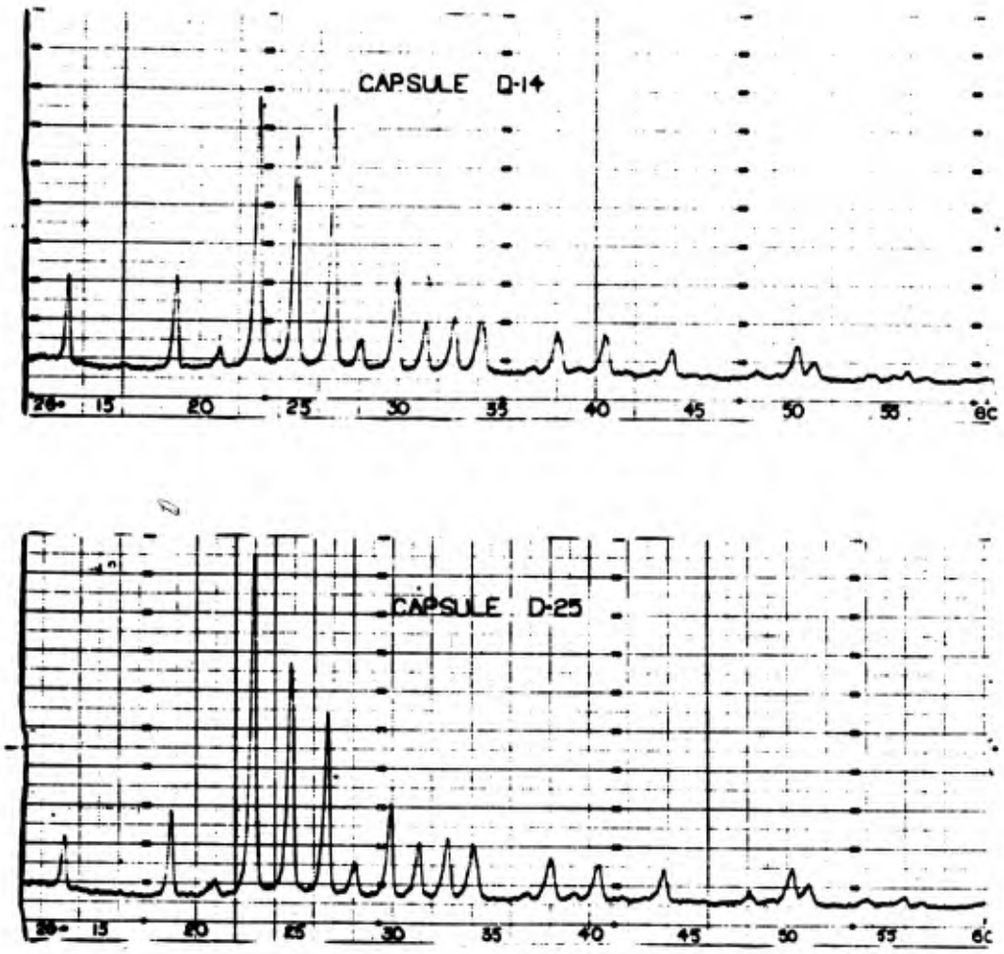

Fig 12 (cont) X-ray diffractograms for irradiated and standard PETN

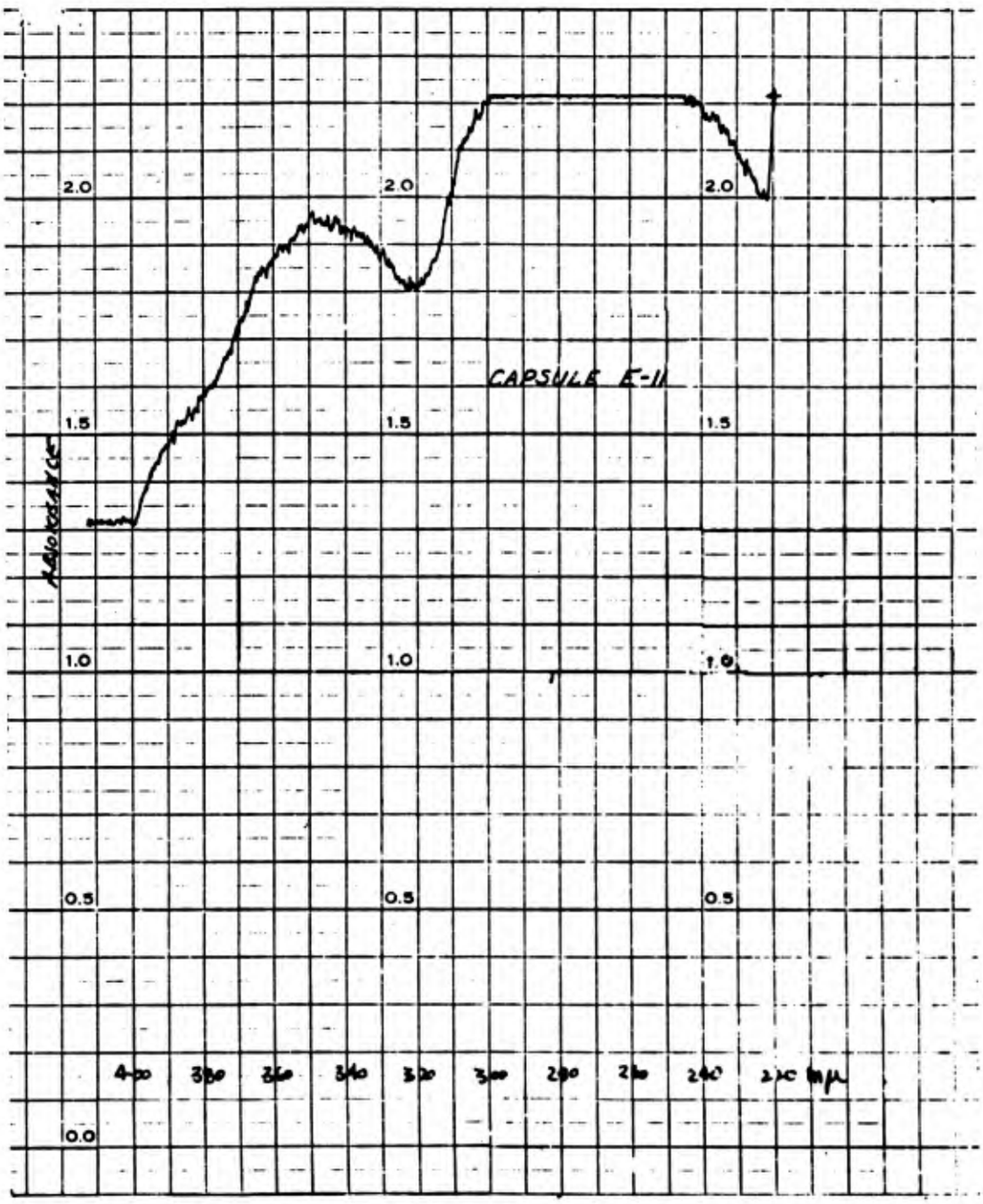

Fig 13a Ultraviolet spectrum for irradiated propellant, Sample (capsule) E11

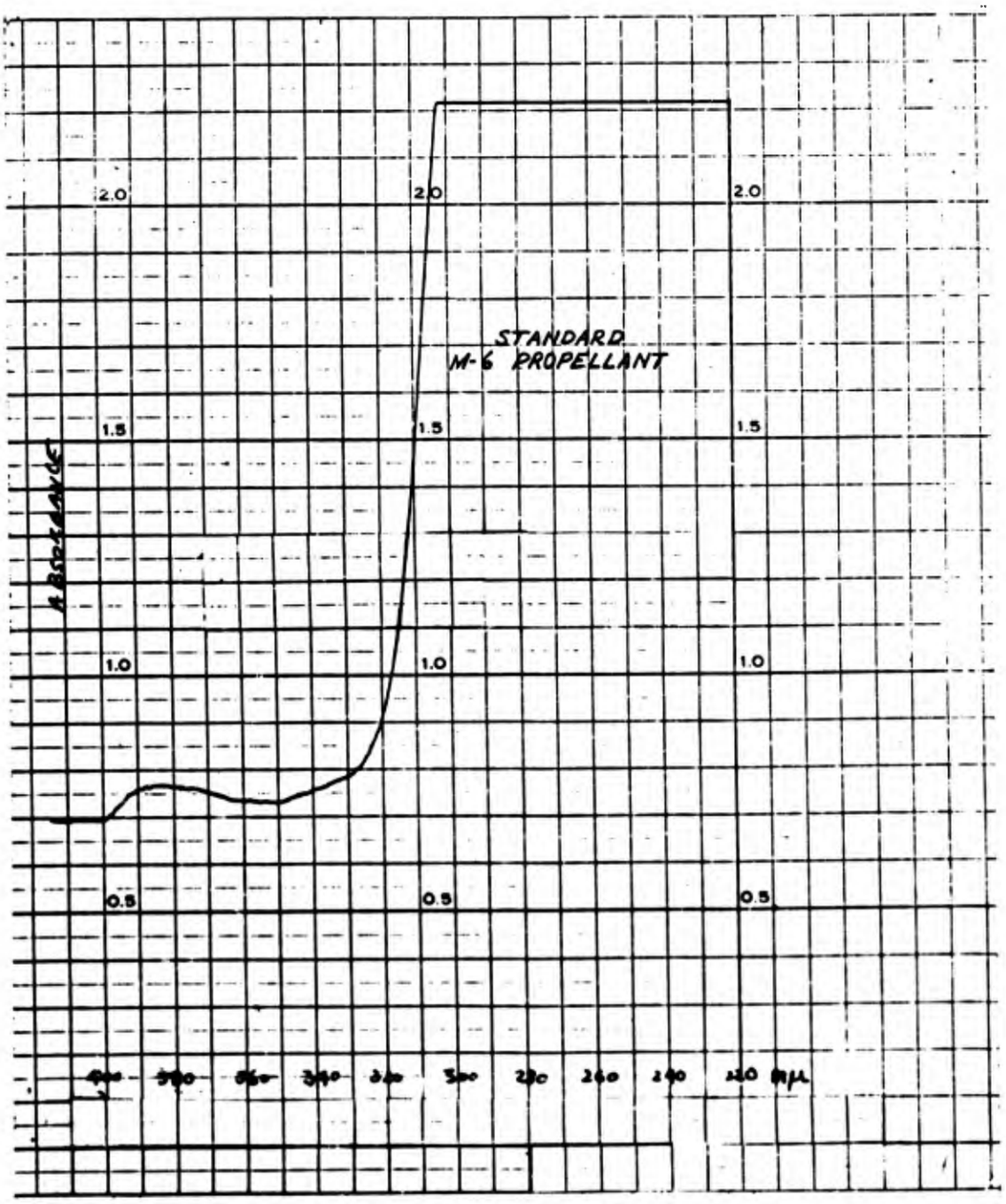

Fig 13b Ultraviolet spectrum for standard propellant, M-6

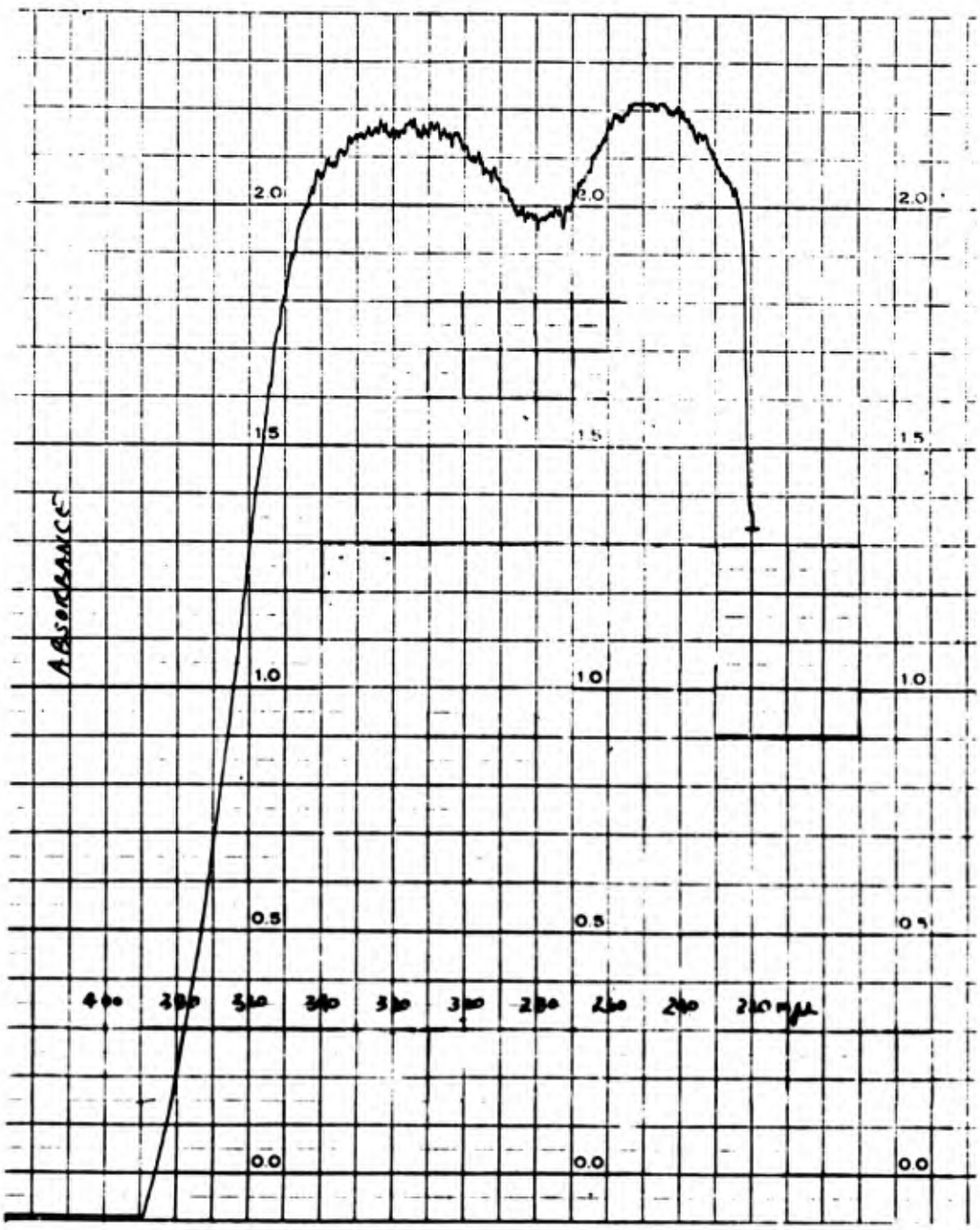

Fig 13c Ultraviolet spectrum for irradiated propellant, Sample (capsule) F22

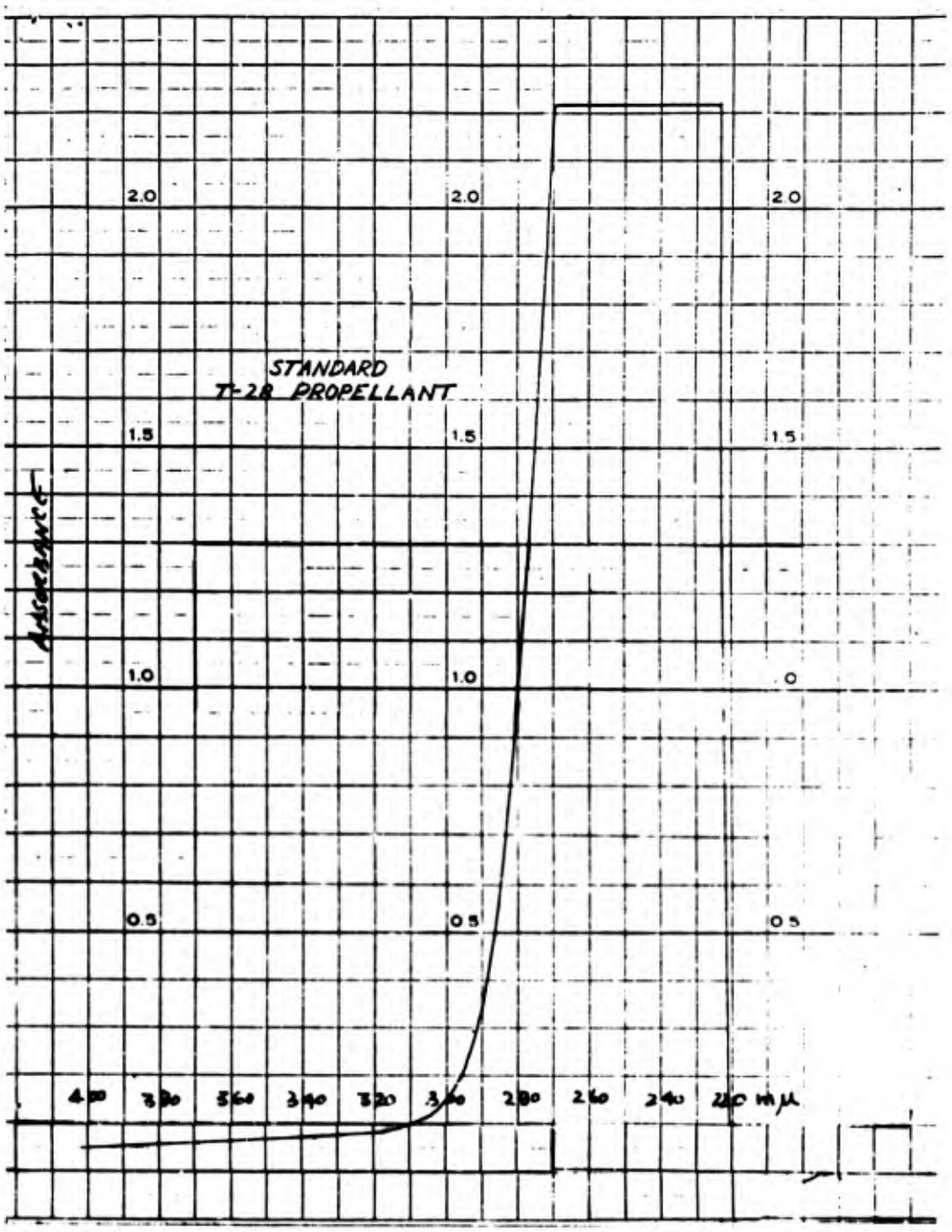

Fig 13d Ultraviolet spectrum for standard propellant, T28

UNCLASSIFIED

Security Classification

DOCUMENT CONTROL DATA - R & D

(Security classification of title, body of abstract and indexing annotation must be entered when the overall report is classified)

1. ORIGINATING ACTIVITY *(Corporate author)*

Picatinny Arsenal, Dover, New Jersey 07885

2a. REPORT SECURITY CLASSIFICATION

Unclassified

2b. GROUP

3. REPORT TITLE

THE EFFECTS OF REACTOR IRRADIATION ON THE CHEMICAL CHARACTERISTICS OF SOLID EXPLOSIVES

4. DESCRIPTIVE NOTES *(Type of report and inclusive dates)*

5. AUTHOR(S) *(First name, middle initial, last name)*

Charles Ribaudo
James Mallay
Harold J. Matsuguma

6. REPORT DATE	7a. TOTAL NO. OF PAGES	7b. NO. OF REFS
January 1970	74	6

8a. CONTRACT OR GRANT NO.	9a. ORIGINATOR'S REPORT NUMBER(S)
b. PROJECT NO	Technical Report 3893
c.	9b. OTHER REPORT NO(S) *(Any other numbers that may be assigned this report)*
d.	

10 DISTRIBUTION STATEMENT

This document has been approved for public release and sale; its distribution is unlimited.

11. SUPPLEMENTARY NOTES	12. SPONSORING MILITARY ACTIVITY

13 ABSTRACT

A study was made of TNT, HMX/EXON (9505), DATB, and PETN which had been irradiated in a nuclear reactor to determine chemical changes induced by the irradiation. Chemical changes (stability) were determined by infrared spectrophotometric, x-ray diffraction, and differential thermal analysis of the post-irradiated explosives. In addition, a similar study of nitrocellulose-base propellants was carried out. From the data obtained, the order of decreasing chemical stability under irradiation was DATB, HMX/EXON, TNT, PETN, and the nitrocellulose-base propellants; DATB was found to be the most stable.

DD FORM 1 NOV 65 1473 REPLACES DD FORM 1473, 1 JAN 64, WHICH IS OBSOLETE FOR ARMY USE.

UNCLASSIFIED

Security Classification

14. KEY WORDS	LINK A		LINK B		LINK C	
	ROLE	WT	ROLE	WT	ROLE	WT
Reactor irradiation						
Solid explosives						
Propellants						
TNT						
HMX/EXON						
DATB						
PETN						
Infrared spectrophotometry						
X-ray diffraction						
Differential thermal analysis						
Chemical stability						
Ultraviolet spectrophotometry						